

**NASA TECHNICAL MEMORANDUM 100548**  
**USAAVSCOM TECHNICAL MEMORANDUM 88-B-009**

**TOWARDS A DAMAGE TOLERANCE  
PHILOSOPHY FOR COMPOSITE MATERIALS  
AND STRUCTURES**

{NASA-TM-100548} TOWARDS A DAMAGE TOLERANCE  
PHILOSOPHY FOR COMPOSITE MATERIALS AND  
STRUCTURES (NASA) 63 p CSCL 11D

N88-22949

Unclas  
G3/24 0142689

**T. KEVIN O'BRIEN**

**MARCH 1988**

**NASA**

National Aeronautics and  
Space Administration

Langley Research Center  
Hampton, Virginia 23665



US ARMY  
AVIATION  
SYSTEMS COMMAND  
AVIATION R&T ACTIVITY

## SUMMARY

A Damage-threshold/Fail-safety approach is proposed for ensuring that composite structures are both sufficiently durable for economy of operation, as well as adequately fail-safe or damage tolerant for flight safety. Matrix cracks are assumed to exist throughout the off-axis plies. Delamination onset is predicted using a strain energy release rate characterization. Delamination growth is accounted for in one of three ways: either analytically, using delamination growth laws in conjunction with strain energy release rate analyses incorporating delamination resistance curves; experimentally, using measured stiffness loss; or conservatively, assuming delamination onset corresponds to catastrophic delamination growth. Fail-safety is assessed by accounting for the accumulation of delaminations through the thickness. A tension fatigue life prediction for composite laminates is presented as a case study to illustrate how this approach may be implemented. Suggestions are made for applying the Damage-threshold/Fail-safety approach to compression fatigue, tension/compression fatigue, and compression strength following low velocity impact.

Keywords: Damage Tolerance, Threshold, Fail-safe, Composite Materials, Delamination, Impact, Fatigue, Compression, Strain Energy Release Rate, Fracture Mechanics

## NOMENCLATURE

A	Coefficient in power law for delamination growth
a	Delamination size
b	Laminate half-width
c	uncracked ply thickness
d	cracked ply thickness
E	Axial modulus of a laminate
$E_{LAM}$	Axial modulus before delamination
$E^*$	Modulus of an edge delaminated laminate
$E_{LD}$	Modulus of a locally delaminated cross section
$E_{LD}^*$	Modulus of local cross section with edge and local delaminations
$E_0$	Initial modulus ( $N=10^0$ cycles)
$E_{11}$	Lamina modulus in the fiber direction
$E_{22}$	Lamina modulus transverse to the fiber direction
$G_{12}$	In-plane shear modulus
G	Strain energy release rate
$G_I$	Mode I strain energy release rate
$G_{II}$	Mode II strain energy release rate
$G_c$	Critical value of G at delamination onset
$G_{max}$	Maximum G in fatigue cycle
$K_\epsilon$	Strain concentration factor

$l$  Laminate length  
 $M$  Number of sublaminates formed by edge delamination  
 $m$  Slope of  $G$  versus  $\log N$  curve for delamination onset  
 $n$  Exponent in power law for delamination growth  
 $N$  Number of fatigue cycles  
 $N_F$  Cycles at failure in fatigue  
 $p$  Number of local delaminations through the laminate thickness  
 $R$  Cyclic stress ratio in fatigue ( $\sigma_{\min}/\sigma_{\max}$ )  
 $2s$  Matrix crack spacing  
 $t$  Thickness  
 $t_{LAM}$  Laminate thickness  
 $t_{LD}$  Thickness of a locally delaminated cross section  
 $\epsilon$  Uniaxial strain  
 $\epsilon_c$  Critical strain at delamination onset  
 $\epsilon_F$  Strain at failure  
 $\epsilon_{\max}$  Maximum strain in fatigue cycle  
 $\sigma$  Uniaxial stress  
 $\sigma_{\max}$  Maximum stress in fatigue cycle  
 $\sigma_{\min}$  Minimum stress in fatigue cycle  
 $\sigma_{alt}$  Alternating Stress in fatigue cycle

## INTRODUCTION

As composite materials are considered for primary structural applications, concern has been raised about their damage tolerance and long term durability. The threat of barely visible, low velocity impact damage, and its influence on compression strength, has surfaced as the most immediate concern for primary structural components such as composite wings [1]. Recent government programs have focused heavily on this issue in developing damage tolerance criteria that will satisfy the safety requirements of current military aircraft [2,3]. At the same time, research has been conducted on low velocity impact; both in the prediction of damage accumulation during the impact [4,5], and in the assessment of the influence of impact damage on compression strength [6-13]. Several methods for improving the performance of impacted composite panels and components have been proposed. One approach is to increase the inherent toughness of the composite by using tougher resin matrices, such as toughened epoxies [9] and thermoplastics [10], or to modify the form of the material by adding tough adhesive layers during the layup or as interleaves in the prepreg [12]. In terms of wing skin design, the goal has been to increase the compression failure strain after impact above the strength of a comparable laminate with an open hole [6,7]. Although this goal may be achieved using clever structural design and the improvements in materials cited, other issues have yet to be adequately addressed.

Although compression strength is greatly reduced after low velocity impact, any further reduction with subsequent fatigue cycles is minimal. Hence, impacted composite panels have very flat compression S-N curves [1,6,13]. This observation has resulted in damage tolerance criteria for composite structures

that require only static loading [2]. However, for toughened matrix composites, where the compression strength after low velocity impact exceeds the strength of the laminate with an open hole, a static criteria may no longer be sufficient. The compression S-N curve for composite laminates with an open hole is not flat, even for toughened matrix composites [14], because the interlaminar stresses at the hole boundary cause delaminations that form in fatigue and grow with increased cycles [15]. Furthermore, other sources of delamination (straight edges, ply drops, matrix cracks) may exist in wing skins and other composite primary structures, such as composite rotor hubs [16]. Although delamination may not cause immediate failure of these composite parts, it often precipitates component repair or replacement, which inhibits fleet readiness, and results in increased life cycle costs. Furthermore, delaminations from several sources may accumulate, eventually leading to catastrophic fatigue failures.

In metallic structures, damage tolerance has been demonstrated using fracture mechanics to characterize crack growth under cyclic loading for the constituent materials, predict the rate of crack growth in the structure under anticipated service loads, and establish inspection intervals and nondestructive test procedures to ensure fail safety. Because composite delamination is a commonly observed damage mechanism in laminated composite structures, many efforts have been undertaken to develop similar procedures for composite materials by characterizing delamination growth using fracture mechanics [17-20]. Although this approach is promising, there are some fundamental differences in the way fracture mechanics characterization of delamination in composites may be used to demonstrate fail safety compared to the classical damage tolerance treatment used for metals.

Previously, a Damage-threshold/Fail-safety approach to composite damage tolerance was proposed as an alternative to the classical approach used for

metals [21]. The purpose of the current paper is to expand on this concept by demonstrating how a Damage-threshold/Fail-safety approach may be used to predict the tension fatigue life of composite laminates, and then illustrating the similarities between this application and the use of the same philosophy for predicting compression fatigue life and compression strength after low velocity impact.

#### DELAMINATION CHARACTERIZATION

Many papers have been published recently where the rate of delamination growth with fatigue cycles,  $da/dN$ , has been expressed as a power law relationship in terms of the strain energy release rate,  $G$ , associated with delamination growth [17-20]. This fracture mechanics characterization of delamination growth in composites is analagous to that of fatigue crack growth in metallic structures, where the rate of crack growth with cycles is correlated with the stress intensity factor at the crack tip. However, delamination growth in composites occurs too rapidly over a small range of load, and hence  $G$ , to be incorporated into a classical damage tolerance analysis for fail safety [18,21,22]. Where in metals the range of fatigue crack growth may be described over as much as two orders of magnitude in  $G$ , the growth rate for a delamination in a composite is often characterized over barely one order of magnitude in  $G$ . Hence small uncertainties in applied load may yield large (order of magnitude) uncertainties in delamination growth rates.

Different damage mechanisms may also interact with the delamination and increase the resistance to delamination growth. Delamination growth resistance curves may be generated to characterize the retardation in delamination growth from other mechanisms [23-25]. These delamination resistance curves are

analogous to the R-curves generated for ductile metals that account for stable crack growth resulting from extensive plasticity at the crack tip. However, unlike crack tip plasticity, other composite damage mechanisms, such as fiber bridging and matrix cracking, do not always retard delamination growth to the same degree. Hence, the generic value of such a characterization is questionable.

One alternative to using the classical damage tolerance approach for composites as it is used for metals would be to use a strain energy release rate threshold for no delamination growth and design to levels below this threshold for infinite life. Metals are macroscopically homogeneous, and the initial stress singularities that create cracks at particular locations in preferred directions cannot be easily identified. Composites, however, are macroscopically heterogeneous, with stiffness discontinuities that give rise to stress singularities at known locations such as straight edges, internal ply drops, and orthogonal matrix cracks. Although these singularities are not the classical  $r^{-1/2}$  variety observed at crack tips, and hence cannot be characterized with a single common stress intensity factor, they can be characterized in terms of the strain energy release rate,  $G$ , associated with the eventual delamination growth.

The most common technique for characterizing delamination onset in composite materials is to run cyclic tests on composite specimens, where  $G$  for delamination growth is known, at maximum load or strain levels below that required to create a delamination under monotonic loading. A strain energy release rate threshold curve for delamination onset may be developed by running tests at several maximum cyclic load levels and plotting the cycles to delamination onset versus the maximum cyclic  $G$ , corresponding to the maximum cyclic load or strain applied [26-30]. This  $G$  threshold curve may then be used



to predict delamination onset in other laminates of the same material, or from other sources in the same laminate [31].

#### DAMAGE-THRESHOLD/FAIL-SAFETY APPROACH

One concern with a no-growth threshold design criteria for infinite life has been the uncertainty inherent in predicting service loads, which could lead to G values that exceed no-growth thresholds and result in catastrophic propagation. This concern is paramount for military aircraft and rotorcraft, where original mission profiles used to establish design loads are often exceeded once the aircraft is placed in service. However, unlike crack growth in metals, catastrophic delamination growth does not necessarily equate to structural failure. In situations where the structure experiences predominantly tensile loads, such as composite rotor hubs and blades, delaminated composites may have inherent redundant load paths that prevent failure and provide a degree of fail safety [21]. This degree of fail safety has led some designers to think of composite delamination as a benign failure mode. Unfortunately, delaminations may occur from several sources in a given component or structure. When this occurs, an iterative composite mechanics analysis that considers each of these potential sites must be performed to ensure fail safety of the structure.

Previously, a Damage-threshold/Fail-safety approach for composite fatigue analysis was proposed [21] that involved the following steps:

- (1) Predict delamination onset thresholds using fracture mechanics
- (2) Assume complete propagation occurs immediately after the delamination threshold is exceeded

(3) Determine the remaining load carrying capability of the composite with delamination present using composite mechanics (i.e., check for fail safety)

(4) Iterate on steps 1-3 to account for multiple sources of delamination

This type of analysis need only be applied to primary structures. However, step 1 may be used to demonstrate the delamination durability of any composite structure by providing an assessment of component repair or replacement costs over anticipated structural service lives. Step 2 reflects a conservative way to deal with the rapid delamination growth rates observed relative to metals as discussed earlier. An alternative to step 2 would be to predict delamination growth rates using growth laws that incorporate R-curve characterizations, thereby taking into account the resistance provided by other damage mechanisms. Such a characterization has been attempted previously [25], but should be used with caution because it is no longer truly generic. A third approach is to monitor stiffness loss in real time, and hence reflect the consequence of delamination growth, and other damage mechanisms, as they occur. This technique was used to predict the tension fatigue life of composite laminates [31], and is summarized in the next section to provide a specific case study for the implementation of the Damage-threshold/Fail-safety approach. However, in most structural applications real-time monitoring of stiffness loss may not be practical, so the conservative approach outlined in step 2 would be applied. Step 3 acknowledges that the residual strength of the composite is a function of structural variables, and is not uniquely a question of material characterization. Hence, the Damage-threshold/Fail-safety concept offers both the benefits of generic material characterization using fracture mechanics,

while reflecting the unique structural character of laminated composite "materials."

## LAMINATE FATIGUE LIFE PREDICTION: A CASE STUDY

### Tension Fatigue Behavior

Figure 1 shows the tension fatigue damage in  $(45/-45/0/90)_s$  X751/50 E-glass epoxy laminates that were subjected to cyclic loading at a frequency of 5 Hz and an R ratio of 0.1 [31]. Figure 2 shows a schematic of some of this damage, including edge delaminations that form at the edge in the 0/90 interface and jump through 90 degree ply cracks to the other 0/90 interface, and local delaminations that form in the 45/-45 interface, originating at 45 degree matrix ply cracks. These same damage mechanisms have been observed in graphite epoxy laminates with the same layup [27,35]. The fatigue damage in the glass epoxy laminates progressed in the following sequence as they were tested at maximum cyclic stress levels below their static strength. First, extensive matrix cracking developed in the 90 degree plies, followed by edge delamination in the 0/90 interfaces. Next, matrix cracks appeared in the 45 degree and -45 degree plies and initiated local delaminations, first in the 45/-45 interfaces, followed by the -45/0 interfaces. Finally, after enough local delaminations had formed through the thickness at a particular location, fiber failure occurred and the laminate fractured.

Fig. 3 shows the number of cycles at a given maximum cyclic stress for edge delaminations to form (solid symbols), for the first local delamination to form at the 45/-45 interface (brackets), and for fatigue failure to occur (open symbols). Under monotonic loading, matrix cracks formed in the 90 degree plies,

followed by edge delaminations in the 0/90 interfaces (solid symbols), and finally, by fiber fracture (open symbols). In order to predict the ultimate fatigue failure of these laminates, the onset and growth of the damage observed must be characterized, and the influence of this damage on laminate stiffness and strength must be determined. Once these relationships are known, fatigue life may be predicted using the the Damage-threshold/Fail-safety approach.

#### Influence of Damage on Laminate Stiffness

Fig. 4 shows the influence of damage on laminate stiffness. As matrix cracks accumulate, and as delaminations form and grow, the stiffness of the laminate decreases. Laminate stiffness is the ratio of the remote stress to the global strain in the laminate. The global strain is typically measured using an extensometer or LVDT (fig.4), which yields the displacement of the laminate over a fairly long gage length relative to the laminate's length. As damage forms and grows in the laminate under a constant maximum cyclic stress, corresponding to a constant applied maximum cyclic load, the global strain in the laminate increases.

Previous studies have determined the relationships between stiffness loss and damage extent [23,32-35]. The amount of stiffness loss associated with matrix cracking depends upon the ply orientation of the cracked ply, the laminate layup, the relative moduli of the fiber and the matrix, and the crack spacing, or density of cracks, in the ply. For example, in ref.33, an equation was derived for stiffness loss due to matrix cracking in the 90 degree plies of cross ply laminates as

$$E = \frac{E_{LAM}}{1 + (1/\lambda s)(c/d)(E_{22}/E_{11})\tanh(\lambda s)} \quad (1)$$

where

$$\lambda = \left( \frac{3G_{12}(c+d)E_{LAM}}{c^2dE_{11}E_{22}} \right)^{1/2} \quad (2)$$

and c and d are the thicknesses of the cracked and uncracked plies, respectively. As the crack density increases, i.e., as the crack spacing, 2s, decreases, the stiffness of the laminate will decrease.

The amount of stiffness loss due to delamination also depends on the laminate layup and the relative moduli of the fiber and the matrix, as well as the location and extent of the delamination. As delaminations form and grow in a particular interface, the laminate stiffness decreases as the delamination size, a, increases. In ref.23, an equation was derived for the stiffness loss associated with edge delamination as

$$E = (E^* - E_{LAM})a/b + E_{LAM} \quad (3)$$

where a/b is the ratio of the delamination size to the laminate half-width, and  $E^*$  is determined from a rule of mixtures expression

$$E^* = \sum_{i=1}^M \frac{E_i t_i}{t} \quad (4)$$

where the moduli of the M sublaminates formed by the delamination,  $E_1$ , are calculated from laminated plate theory. The difference in  $E_{LAM}$  and  $E^*$  reflects the loss of transverse constraint in the sublaminates formed by the delamination.

Delaminations starting from matrix cracks will affect laminate stiffness differently than delaminations growing from the straight edge. In ref.32, an equation was derived for the stiffness loss associated with delaminations from matrix cracks as

$$E = \left( (a/l)t_{LAM} \left( \frac{1}{t_{LD}} E_{LD} - \frac{1}{t_{LAM}} E_{LAM} \right) \right)^{-1} \quad (5)$$

where  $a/l$  is the ratio of the delamination length to the laminate length, and  $E_{LD}$  and  $t_{LD}$  represent the modulus and thickness of the locally delaminated region in the vicinity of the matrix crack. The locally delaminated modulus,  $E_{LD}$ , is calculated using laminated plate theory and is similar to  $E^*$  in eq(4). However, in addition to reflecting the loss in transverse constraint due to the delamination,  $E_{LD}$  also reflects the loss of the load bearing capacity of the cracked ply. Similar to edge delamination, the stiffness of the laminate decreases as the size of the delamination increases. However, unlike edge delaminations, which form at the two edges and grow progressively towards the center of the laminate width, local delaminations tend to accumulate at several matrix cracks along the length, growing only a small distance at any one location. The cumulative effect of these local delaminations with cycles, however, may have a significant effect on measured stiffness loss.

## Delamination Onset and Growth Characterization

In order to predict stiffness loss as a function of fatigue cycles, the onset and growth of matrix cracks and delaminations must be characterized. This characterization should be done using a generic parameter that is representative of the composite material being tested, but independent of laminate structural variables such as layup, stacking sequence, and ply thickness. Typically, the strain energy release rate,  $G$ , associated with matrix cracking and delamination is used for this purpose.

Fig. 5 shows the steps that would be required to predict stiffness loss as a function of fatigue cycles using a  $G$  characterization of damage onset and growth. First, plots of  $G$  versus  $\log N$  must be generated to characterize the onset of delamination [21,28,31], and power law relationships between  $G$  and the rate of growth of delamination with fatigue cycles are needed to characterize damage growth [17-20,22] (fig. 5a). Similar approaches may be used to characterize the onset and growth of matrix cracks [33]. Using these material characterizations, the decrease in matrix crack spacing,  $2s$ , and the increase in delamination size,  $a$ , with fatigue cycles may be predicted (fig.5b). This information, in turn, may be used with eqs(1-5) to predict the decrease in modulus with cycles, which for a constant stress amplitude test is tantamount to predicting the increase in global strain with cycles (fig.5c).

Although this technique may be demonstrated for cases where there is one dominant damage mechanism, application of this approach in general is difficult because the various damage modes interact, complicating their unique characterization in terms of  $G$  [33]. For example, although the elastic analysis for  $G$  associated with edge delamination growth is independent of delamination

size, stable delamination growth is often observed experimentally [23,25]. The strain energy release rate for edge delamination was derived in ref.23 as

$$G = \frac{\epsilon^2 t_{LAM}}{2} (E_{LAM} - E^*) \quad (6)$$

which is independent of the delamination size. Theoretically, when a critical value of strain,  $\epsilon_c$ , is reached, corresponding to a critical  $G_c$ , the delamination should grow catastrophically across the laminate width. However, edge delaminations usually grow in a stable fashion, requiring increasing strain levels, and hence increasing  $G$ , for the delamination to grow across the width. This stable growth may be correlated with the accumulation of 90 degree matrix cracks ahead of the delamination front. For example, fig.6 shows a plot of normalized delamination size,  $a/b$ , as a function of the strain applied to an eleven-ply ( $\pm 30/\pm 30/90/90$ )<sub>s</sub> T300/5208 graphite epoxy laminate [23]. The edge delaminations form at a strain of approximately 0.0035, but do not grow across the specimen width until the strain reaches approximately 0.0065. Also plotted in fig.6 on the right hand ordinate is the 90 degree ply crack spacing measured in the center of the laminate. There appears to be a direct correlation between the stable delamination growth and the accumulation of matrix cracks ahead of the delamination front. These matrix cracks apparently alter the local stress state at the delamination front and increase the resistance to delamination growth. Stable delamination growth may be predicted by generating a delamination resistance R-curve using eq.6 [23,25]. However, the resulting R-curve is no longer generic, because the matrix cracking that is causing the delamination resistance is governed by structural variables such as ply thickness and stacking sequence.



Delamination also influences the formation and accumulation of matrix cracks. Delamination relaxes the constraint of neighboring plies, and hence changes the saturation spacing of matrix cracks in the off-axis plies. For example, when delaminations form at the edges of the  $(\pm 30/\pm 30/90/90)_s$  laminate shown in fig. 6, the constraint between the -30 deg and 90 deg plies is relaxed, and the 90 deg cracks form at lower strain levels, with smaller crack spacings, than possible if no delamination had existed [23]. An R-curve description of matrix cracking has been used to describe the accumulation of matrix cracks, similar to the approach that has been attempted for delamination [33]. However, when these cracks interact with delaminations, this description is no longer generic.

Even if one could achieve a truly generic description of damage accumulation with cycles, the resulting stiffness loss prediction, and hence the prediction of increasing global strain with cycles, is necessary, but not sufficient, to predict fatigue life. The final failure of the laminate is governed not only by loss in stiffness, but also by the the local strain concentrations that develop in the primary load bearing plies, which in most laminates are zero degree plies.

#### Influence of Local Strain Concentrations on Failure

Fig. 7a shows that fatigue failures typically occur after the global strain has increased because of the fatigue damage growth, but before this global strain reaches the global strain at failure,  $\epsilon_F$ , measured during a static strength test [27,31,34,35]. Therefore, local strain concentrations must be present in the zero degree plies that control the laminate strength. Although matrix cracks create small strain concentrations in the neighboring plies, their

magnitudes are generally small because the stiffness of the cracked ply is usually much less than the stiffness of the zero degree ply [36]. Furthermore, strain concentrations due to matrix cracks act over only a local volume in the adjacent ply near the crack tip [36]. Hence, the final failure in a zero degree ply of a laminate may follow a neighboring ply crack [37], but the laminate failure strain will not be strongly influenced by the presence of the matrix cracking [36]. However, once delaminations initiate at matrix ply cracks anywhere through the laminate thickness, the local strain will increase significantly in all of the remaining uncracked plies [21,27,32,34-36]. These local strain increases may not be sensed by the global strain measurement, because delaminations starting from matrix cracks grow very little once they form. If several delaminations form at matrix cracks throughout the laminate thickness at one location, then the local strain on the zero degree plies at that location may reach the static failure strain, resulting in the observed fatigue failure (fig.7b).

This mechanism for fatigue failure has been observed previously for graphite epoxy laminates [27,34,35], and the local strain concentrations resulting from cumulative local delaminations through the thickness have been quantified [21,27,32,34,35]. These local strain concentrations may be calculated as

$$K_{\epsilon} = \frac{E_{LAM} t_{LAM}}{E_{LD} t_{LD}} \quad (7)$$

Typically, the local strain concentration will result in a trade off between the increased modulus,  $E_{LD} > E_{LAM}$ , because  $E_{LD}$  is a more zero degree dominated layup

than the original laminate, and the decrease in load bearing cross section,  $t_{LD} < t_{LAM}$ .

Each time a delamination initiates from a matrix crack, the local strain in the remaining uncracked plies, and hence in the zero degree plies, increases by an amount equal to  $K_\epsilon$  times the global cyclic strain,  $\epsilon_{max}$ , until it reaches the static failure strain,  $\epsilon_F$ , (fig. 8a). A simpler way to visualize this process, however, is to reduce the static failure strain to some effective global failure strain,  $(\epsilon_F)_i$ , each time a new local delamination forms through the thickness. Hence,  $(\epsilon_F)_i$  would be equal to  $\epsilon_F / (K_\epsilon)_i$ . As local delaminations accumulate through the thickness, the effective failure strain would decrease incrementally. Because  $(K_\epsilon)_i$  reflects the strain concentration resulting from accumulated local delaminations through the laminate thickness, fatigue failure would correspond to the number of cycles where the damage growth increased the global maximum cyclic strain,  $\epsilon_{max}$ , to the current value of  $(\epsilon_F)_i$  (fig. 8b). This approach does not require a prediction of damage growth with fatigue cycles if the laminate stiffness loss, and hence the increase in global strain, can be monitored in real time. When this is possible, only the incremental decrease in the effective failure strain needs to be predicted to predict fatigue life. This may be accomplished by assuming that matrix cracks exist in all of the off-axis plies. This assumption is analogous to assuming the existence of the smallest flaw in a metal that could be detected non-destructively to assess damage tolerance. Then, the number of fatigue cycles to onset of each local delamination through the thickness may be predicted using delamination onset criteria (fig. 5a) along with strain energy release rate analyses for local delamination. As each local delamination forms,  $\epsilon_F$ , may be reduced by the

appropriate  $K_{\epsilon}$  and compared to the current value of  $\epsilon_{\max}$ , based on measured stiffness loss, to determine if fatigue failure will occur. Hence, the ability to predict local delamination onset, and its effect on  $\epsilon_F$ , facilitates using measured stiffness loss to predict fatigue life. However, for many composite structures real-time stiffness measurement may not be practical. In these cases, the conservative approach for step 2 in the Damage-threshold/ Fail-safety approach outlined earlier could be applied.

If the conservative approach was used to predict the tension fatigue life of  $(45/-45/0/90)_S$  laminates, for example, stiffness would decrease incrementally, i.e.,  $\epsilon_{\max}$  would increase incrementally, with the onset of each damage mechanism. Figure 9 shows a sketch for conservative fatigue life prediction in  $(45/-45/0/90)_S$  graphite-epoxy and glass-epoxy laminates. Because matrix cracks are assumed to exist in the off-axis plies,  $\epsilon_{\max}$  is increased in the first load cycle, corresponding to the stiffness loss associated with saturation crack spacing in the off-axis plies. This stiffness loss would be greater for glass epoxy laminates than for graphite epoxy laminates [31]. The influence of matrix cracks on local strains in the zero deg plies will be neglected for the reasons stated earlier. Hence,  $\epsilon_F$  will remain unchanged. When edge delamination occurs in the 0/90 interfaces,  $\epsilon_{\max}$  will increase again, corresponding to complete delamination throughout the laminate width. This stiffness loss would be greater for graphite epoxy laminates than for glass epoxy laminates [31]. However,  $\epsilon_F$  would not change because edge delaminations do not create local strain concentrations in the zero deg plies [32]. As each local delamination forms,  $(\epsilon_F)_i$  will decrease, as determined by  $(K_{\epsilon})_i$ , and  $\epsilon_{\max}$  will increase, corresponding to delamination growth throughout the particular

interface. When enough local delaminations form through the thickness such that  $(\epsilon_{\max})_i \geq (\epsilon_F)_i$ , fatigue failure will occur. These predictions will be conservative because matrix cracking typically does not reach saturation spacing in all of the off-axis plies in the first load cycle, and because delaminations grow rapidly at first, but then are retarded by interaction with matrix cracking, and hence, rarely grow catastrophically.

Because stiffness loss data were available for the glass epoxy laminates in this case study, measured stiffness loss was used to determine the increase in  $\epsilon_{\max}$  with fatigue cycles instead of using the conservative prediction methodology. Furthermore, the G vs. log N delamination characterization was generated using edge delamination data from the  $(45/-45/0/90)_s$  laminates and was then used to predict local delamination onset in these same laminates. Hence, the accuracy of this fatigue life prediction depends primarily on the validity of reducing the failure strain incrementally to account for the accumulation of local delaminations through the laminate thickness. The next section outlines how this fatigue life prediction was performed in the context of the Damage-threshold/ Fail-safety philosophy.

### Life prediction using Damage-threshold/Fail-safety approach

#### Step 1: Delamination onset prediction

In order to predict the onset of local delaminations with fatigue cycles, the G versus log N characterization of the composite material must be generated. This characterization may be accomplished using a variety of interlaminar fracture test methods [22,26,28-30]. Data from several materials with brittle

and tough matrices indicated that between  $10^0 \leq N \leq 10^6$  cycles, the maximum cyclic  $G$  may be represented as a linear function of  $\log N$  (fig.10), where  $N$  is the number of cycles to delamination onset at a prescribed  $G_{\max}$  [28]. Hence,

$$G = m \log N + G_c \quad (8)$$

where  $G_c$  and  $m$  are material parameters that characterize the onset of delamination under static and cyclic loading in the material (fig.5a). A more recent study indicates that for some tough thermoplastic matrix composites, the static toughness is so great compared to the fatigue behavior that a linear representation may not be valid [22]. Furthermore, the static toughness may depend on the loading rate, which would influence the ultimate shape of the curve. For example, if slow monotonic loading is used to measure the static toughness, both  $G_c$  and the slope,  $m$ , may be different from the results plotted using  $G_c$  measured at a load rate that corresponds to the frequency of cyclic loading. Because a low toughness, glass epoxy composite was tested in ref.31, a linear characterization was used in this case study. The static data in ref.31 were measured at a relatively slow rate of 0.5 mm/min.

To predict delamination onset,  $G$  must be calculated for the first local delamination that will form. This typically occurs at a matrix crack in the surface ply, but may be confirmed by calculating  $G$  for matrix cracking in all of the off-axis plies in the laminate. The one with the highest  $G$  for the same applied load will be the first to form. This  $G$  may be calculated using the equation for the strain energy release rate associated with local delaminations initiating at matrix cracks [32]

$$G = \frac{\sigma^2 t_{LAM}^2}{2} \left( 1/t_{LD} E_{LD} - 1/t_{LAM} E_{LAM} \right) \quad (9)$$

To calculate the number of cycles for the first local delamination to form,  $N_1$ , eq(9) for  $G$  is set equal to the delamination onset criterion of eq(8) and then solved for  $N_1$ . Hence,

$$\log N_1 = \frac{1}{m} \left[ \frac{\sigma_{max}^2}{2} t_{LAM}^2 \left( 1/t_{LD} E_{LD} - 1/t_{LAM} E_{LAM} \right) - G_c \right] \quad (10)$$

### Step 2: Assessment of Damage Growth and Stiffness Loss

Delamination growth information is needed to determine the amount of stiffness loss, and hence the increase in global strain, that has occurred by the time the first local delamination has formed at  $N_1$  cycles. In graphite epoxy laminates, the majority of this stiffness loss is associated with delamination; however, in glass epoxy laminates matrix cracking may also contribute significantly to stiffness loss [31]. In either material the interaction of matrix cracking and delamination complicates the prediction of damage growth, and hence the prediction of stiffness loss. Therefore, instead of predicting stiffness loss by predicting the rate of delamination growth and accumulation of matrix cracks with fatigue cycles, stiffness loss was monitored experimentally.

### Step 3: Assessment of fail-safety

The strain concentration associated with the first local delamination,  $(K_\epsilon)_1$ , may be calculated using eq.7. Fatigue failure will occur if the maximum global strain, resulting from the stiffness loss associated with damage growth at  $N_1$  cycles, reaches the effective failure strain when the local delamination forms, which is calculated as  $(\epsilon_F)_1 = \epsilon_F / (K_\epsilon)_1$ . Hence, failure will occur if  $\epsilon_{\max} \geq (\epsilon_F)_1$ . If the first local delamination does not cause failure, then further local delamination sites must be considered.

Step 4: Analysis of multiple local delaminations through the thickness

As shown in fig.11, the thickness and modulus terms in eq(9) change for each successive local delamination that forms through the thickness. For example,  $t_{LD}$  and  $E_{LD}$  for a 45/-45 local delamination in a  $(45/-45/0)_s$  laminate becomes the  $t_{LAM}$  and  $E_{LAM}$  values used for the next local delamination that forms through the thickness. Therefore, as local delaminations accumulate through the thickness under a constant  $\sigma_{\max}$ , the driving force (i.e. G) for each new delamination changes. Hence, fatigue life prediction for composite laminates requires a "cumulative damage" calculation, even for constant amplitude loading. To calculate the number of cycles for each successive local delamination to form,  $N_i$ , the appropriate form of eq(9) for G is set equal to the delamination onset criterion of eq(8) (fig.11) and then solved for  $N_i$  (fig.12). Hence,

$$\log N_i = \frac{1}{m} \left[ \frac{\sigma_{\max}^2}{2} (t_{LAM}^2)_i \left( 1/t_{LD}E_{LD} - 1/t_{LAM}E_{LAM} \right)_i - G_c \right] \quad (11)$$



Fatigue failure will occur when  $\epsilon_{\max} \geq (\epsilon_F)_i$ , with a resulting fatigue life,  $N_F$ , of

$$N_F = \sum_{i=1}^p N_i \quad (12)$$

where  $p$  is the number of local delaminations that form through the thickness of the laminate before failure.

Because of the scatter in the experimental data, the constant load amplitude fatigue life prediction methodology outlined in fig.12 more closely resembles fig.13. The variation in initial laminate modulus (i.e, the variation in  $\epsilon_{\max}$ ) and the variations in the static failure strains from specimen to specimen must be taken into account. Hence, a range of possible fatigue lives would be predicted, rather than a single value. The lowest life would occur when the minimum value of  $(\epsilon_F)_i$  in the  $\epsilon_F$  distribution reaches the largest  $\epsilon_{\max}$  value in the distribution resulting from variations in laminate moduli.

#### Life Prediction for Glass-Epoxy Laminates

The Damage-threshold/Fail-safety approach outlined above was used to predict the fatigue life of (45/-45/0/90)<sub>s</sub> E-glass epoxy laminates [31]. First, the delamination onset behavior in fatigue was characterized in terms of strain energy release rates. The maximum cyclic strain versus cycles to edge delamination onset for the laminate was used in eq(6) and the data were plotted versus log N (fig.14). There was significant scatter in the static data for  $G_c$ , possibly due to the interaction that occurred between the edge delamination as

it formed and the 90 deg ply cracks that were extensive before edge delamination onset [33]. Previous work has demonstrated that  $G_c$  values from edge delamination data may be artificially elevated if extensive 90 degree cracking is present in the laminate [26]. Therefore, the minimum values in fatigue were used in eq(8) to characterize delamination onset. For the X751/50 E-glass epoxy, a  $G_c$  value of 0.56 in-lbs/in<sup>2</sup> was obtained, and the slope,  $m$ , was -0.06.

Figure 15 shows the maximum cyclic strain as a function of fatigue cycles for the (45/-45/0/90)<sub>s</sub> X751/50 E-glass epoxy laminates cycled at a maximum cyclic stress of 210 MPa and an R of 0.1. Also shown in fig.15 is the reduction in effective  $\epsilon_F$  for local delaminations accumulating through the thickness. The range of estimated and measured fatigue lives for several  $\sigma_{max}$  levels is summarized in fig.16. The agreement between predicted and measured fatigue lives is reasonably good.

#### FACTORS AFFECTING DELAMINATION ONSET AND GROWTH

The agreement between measured and predicted fatigue lives in fig.16 indicates that the Damage-threshold/Fail-safety approach, in the form of a through-thickness damage accumulation model, can accurately describe fatigue failure for a material whose delamination behavior in fatigue is well characterized. In this case, the  $G$  vs.  $\log N$  characterization was generated using data from the same laminates whose fatigue lives were being predicted. In general, however, the  $G$  vs.  $\log N$  characterization would be performed on standardized laboratory tests, and then used to predict the fatigue behavior of structural components made of the same material. Hence, the laboratory characterization must be performed on identical materials (same constituents,

fiber volume fraction, cure conditions, etc.) under identical environments (temperature, moisture, etc.) and loading conditions (load rate, R-ratio, frequency, etc.) as the structure for the fatigue life prediction to be accurate. Furthermore, although delamination growth data are difficult to utilize because of steep growth rates and damage mode interactions, these data are useful, nevertheless, to identify how the various material, environment, and loading variables that effect delamination onset will influence delamination growth.

Of the many factors that may affect delamination onset and growth, a few have been studied in detail. For example, the toughness of the matrix will have a very strong effect on  $G_c$  but very little influence on delamination onset at  $10^6$  cycles (fig.10) [26,28-30]. Therefore, the slope,  $m$ , as measured by fitting the delamination onset data to eq(8) will be lower for a brittle matrix composite than a tougher matrix composite (fig.17a) [28]. Assuming that the brittle and tough matrix composites eventually reach a common  $G$  threshold for delamination onset at  $N \geq 10^6$  cycles [22,26,28,29], then the exponent,  $n$ , in a delamination growth law would be lower for the tougher matrix composite (fig.17b) [18].

Delamination characterization may also depend on the mixed-mode ratio for the particular source of delamination. Previous studies have shown that the total  $G_c$  at delamination onset under a monotonic loading varies as a function of the mixed-mode percentage at the delamination front [29,38,39]. The total  $G_c$  will be highest for situations where the mode II component is greater than the mode I component (fig.18a). However, the  $G$  threshold for delamination onset at  $N \geq 10^6$  cycles has been shown to be nearly identical for all mixed mode ratios, from pure mode I to pure mode II [22,26,28,29]. Therefore, as shown in fig.18a,  $m$  in eq(8) will be greater for delaminations that are predominantly due to

interlaminar shear (mode II) than for delaminations that are predominately due to interlaminar tension (mode I). Assuming a common  $G$  threshold for delamination onset at  $N \geq 10^6$  cycles, the exponent in the delamination growth power law would be lowest for the pure mode II case and highest for the pure mode I case (fig.18b). Previous delamination growth studies have verified these trends [17-19]. For the glass epoxy laminate fatigue life prediction summarized earlier, conservative values of  $G_c$  and  $m$  were used in eq(8) because of the scatter in the static total  $G_c$  measured using edge delamination data. Hence, the mixed-mode ratio dependence was ignored. In general, however, the mixed mode dependence on  $G_c$  should be determined for both the material characterization test(s) as well as the delamination source being modeled in the structural component. However, if the long term delamination durability is of primary concern, the  $G$  threshold at  $N \geq 10^6$  cycles is all that is needed. In this case, only a simple total  $G$  analysis is required, since the  $G$  threshold does not depend strongly on the mixed mode ratio. This greatly simplifies the analysis, because total  $G$  may be calculated using relatively simple analyses like eqs(6) and (9) [23,32].

Changing the R-ratio of the cyclic loading will not affect  $G_c$  but may have a significant influence at  $10^6$  cycles (fig.19a) [22,30]. Therefore, the slope,  $m$ , will be greater for lower R-ratios corresponding to greater alternating stress levels. Hence,  $G$  threshold values at  $10^6$  cycles will be lower for smaller R-ratios [30]. Consequently, the exponent of the delamination growth power law will be lower for the lower R-ratios (fig.19b).

The influence of other material, environmental, and loading variables have been examined [24,40,41]. However, most of this work has been performed for

static toughness and/or delamination growth. Much work still needs to be done to determine the influence of these variables on delamination onset.

#### DAMAGE-THRESHOLD/FAIL-SAFETY APPROACH FOR COMPRESSION

In the previous case study, and in the examples cited in ref.21, the Damage-threshold/Fail-safety approach was illustrated for problems that involved only tension loading. However, this same approach may be applied to laminates subjected to compression loading. Delamination onset characterization would be conducted in the same way, with only the assessment of fail safety (step 3) changing significantly.

The significance of accumulated delaminations on compression strength has been documented previously by comparing the strength of laminates with one, two, or three implanted delaminations through the thickness to identical laminates with either barely visible or visible impact damage (fig.20) [42]. These results show that the compression strength for laminates with 2.0 inch diameter implanted delaminations, normalized by the compression strength for the same laminates with a 1/4 inch open hole, decreases as the number of delaminations increases through the thickness. Still lower compression strengths were observed for the impacted laminates, which typically contain delaminations in nearly every interface [11]. Similar studies have compared the residual compression strength of virgin laminates, or laminates that had implanted delaminations in a single interface, to identical laminates without implants that had undergone low velocity impact with subsequent cycling [6,13]. For example, fig.21 shows a plot of cycles to failure as a function of stress amplitude for  $(0/90/0/45/-45/0)_s$  graphite epoxy laminates subjected to fully reversed cyclic loading, either in the initially undamaged state, or following an impact with a

potential energy per unit thickness of 1790 J/m [13]. The data in fig.21 indicate that the compression strength after impact is very low compared to the fatigue behavior of the virgin laminate. Furthermore, most of the strength reduction occurs after the impact, with very little degradation due to subsequent cyclic loading.

For composites loaded in compression, final failure is not necessarily determined by the local strain concentration in the zero degree plies, but often results from a global instability that occurs after delaminations accumulate through the thickness and become locally unstable. For example, fig.22 shows dye penetrant enhanced radiographs of the edge of a 40-ply thick,  $(45/0/-45/90)_{5s}$  T300/3501-6 graphite epoxy laminate, containing Kevlar stitches across the specimen width, that was cycled in compression at a maximum cyclic compression stress of 32.5 Ksi and an R-ratio of 10 [43]. After 320,000 cycles, delaminations had formed at the edge near the top surface. The sublaminates that formed buckled locally, which in turn led to more delaminations forming in adjacent interfaces and subsequently buckling. The accumulation of these delaminations through the thickness eventually reduced the cross section carrying the compression load to the point at which global instability occurred and the laminate fractured. This accumulation of delaminations through the thickness occurred over the last 1000 cycles of the fatigue life. In laminates without through-thickness stitching, this final phase of the fatigue life may be even more rapid, and very difficult to document. In these situations, where the accumulation of delamination through the thickness occurs rapidly, prediction of the initial delamination onset may provide a reasonable estimate of fatigue life in addition to establishing the delamination durability of the composite.

Because of this progressive buckling mode of failure, compression fatigue lives are typically much lower than tension fatigue lives for identical

laminates subjected to identical load amplitudes [13]. Combined tension/compression fatigue lives may be reduced even further as a result of delaminations forming from matrix cracks under tension loads and then growing as a result of local instabilities under the compression loads [44]. In each case, however, the final failure results from an accumulation of delaminations through the thickness. The Damage-threshold/Fail-safety approach could be used to estimate fatigue lives in each case. First, delamination onset would be predicted using the appropriate analysis for  $G$  in eq.(8) depending upon the source of the original delamination. Next, delaminations would be assumed to grow throughout the interface immediately, or solutions for instability driven delamination growth in compression would have to be incorporated if stiffness loss could not be monitored directly in real time. Several fracture mechanics models have been developed for the growth of through-width and elliptical patch delaminations in a single interface [45-49]. These analyses would have to be extended to model laminates with multiple edge delaminations to simulate compression fatigue damage, and laminates with multiple delaminations that were formed by matrix cracks to simulate tension/compression fatigue damage. Finally, fail safety may be assessed in compression, as delaminations form near the surface and then accumulate through the thickness, using appropriate models for local and global buckling of the damaged laminate.

These same models could be used to evaluate the consequence of low velocity impact damage. Previous studies have shown that low velocity impact damage develops as extensive matrix cracking and associated delaminations through the thickness [10-12]. Delamination onset in these cases has been modeled as delaminations initiating from matrix cracks under bending loads [50]. In brittle matrix composites, impacts that are barely visible on the impacted surface may be extensive not only on the back surface, but throughout the laminate

thickness. This extensive delamination results in greatly reduced compression strength. Subsequent cyclic loading may create only slightly greater damage growth, which would explain the relatively flat S-N curves observed for impacted brittle matrix laminates (fig.21). Tougher matrix composites, however, suppress some of the delaminations that would otherwise form through the thickness during the impact [10]. Therefore, the compression strength following impact is greater than the compression strength for similar laminates with brittle matrices, but subsequent cyclic loading may cause further damage and corresponding reductions in residual compression strength. In either case, the Damage-threshold/Fail-safety approach may be used to characterize the delamination onset and assess the fail safety of the damaged laminate.

#### SUMMARY

- ⊙ A Damage-threshold/Fail-safety approach was proposed to ensure that composite structures are both sufficiently durable for economy of operation, as well as adequately fail safe or damage tolerant for flight safety. This approach involved the following steps:
  - 1) Matrix cracks are assumed to exist throughout the off-axis plies
  - 2) Delamination onset is predicted using a strain energy release rate characterization
  - 3) Delamination growth is accounted for in one of three ways:
    - ⊙ Analytically, using delamination growth laws in conjunction with strain energy release rate analyses incorporating delamination resistance curves
    - ⊙ Experimentally, using measured stiffness loss



⊙ Conservatively, assuming delamination onset corresponds to catastrophic delamination growth.

4) Fail-safety is assessed by accounting for the accumulation of delaminations through the thickness.

⊙ A tension fatigue life prediction for glass epoxy laminates was presented as a case study to illustrate how the Damage-threshold/Fail-safety approach may be implemented. A fracture mechanics analysis of edge delamination was used to generate a delamination onset criterion for the material. Then, strain energy release rates were calculated for local delaminations that formed at matrix ply cracks through the laminate thickness, and were compared to the criterion to predict local delamination onset. Delamination growth was accounted for experimentally using measured stiffness loss. Finally, fail safety was determined by accounting for the local strain concentration on the zero degree plies resulting from delaminations forming at matrix cracks through the laminate thickness.

⊙ Suggestions were made for applying the Damage-threshold/Fail-safety approach to compression fatigue, tension/compression fatigue, and compression strength following low velocity impact. In all of these analyses, strain energy release rates may be used to predict delamination onset, and fail safety may be assessed by accounting for the effect of delaminations that have accumulated through the thickness.

## REFERENCES

1. O'Brien, T.K., "Interlaminar Fracture of Composites," J. of the Aeronautical Society of India, Vol. 37, No.1, Feb. 1985, pp. 61-70.
2. Demuts, E., Whitehead, R.S., and Deo, R.B., "Assessment of Damage Tolerance in Composites," Composite Structures, Vol.4, 1985, pp. 45-58.
3. Rogers, C., Chan, W., and Martin, J., "Design Criteria for Damage-Tolerant Helicopter Primary Structure of Composite Materials," Vol.1-3, USAAVSCOM TR-87-D-3B, June, 1987.
4. Bostaph, G.M., and Elber, W., "A Fracture Mechanics Analysis for Delamination Growth During Impact on Composite Plates," in Advances in Aerospace Structures, Materials, and Dynamics: A Symposium on Composites, ASME Winter Annual Meeting, Nov. 1983, pp. 133-138.
5. Shivakumar, K.N., Elber, W., and Illg, W., "Prediction of Low Velocity Impact Damage in Thin Circular Plates," AIAA Journal, Vol. 23, No.3, March, 1985, p.442.
6. Byers, B.A., "Behavior of Damaged Graphite/Epoxy Laminates under Compression Loading," NASA CR 159293, Aug. 1980.
7. Starnes, J.H., Rhodes, M.D., and Williams, J.G., "Effects of Impact Damage and Holes on the Compression Strength of a Graphite Epoxy Laminate," in Nondestructive Evaluation and Flaw Criticality for Composite Materials, ASTM STP 696, 1979, pp. 145-171.
8. Starnes, J.H., and Williams, J.G., "Failure Characteristics of Graphite-Epoxy Structural Components Loaded in Compression," in Mechanics of Composite Materials, Z. Hashin and C.T. Herakovich, eds., Pergamon Press, 1982, pp. 283-306.

9. Williams, J.G., O'Brien, T.K., and Chapman, A.C., " Comparison of Toughened Composite Laminates using NASA Standard Damage Tolerance Tests," in Selected Research in Composite Materials and Structures, NASA CP 2321, Proceedings of the ACEE Composite Structures Technology Conference, Seattle, WA, August, 1984.
10. Carlile, D.R., and Leach, D.C., "Damage and Notch Sensitivity of Graphite/PEEK Composite," Proceedings of the 15th National SAMPE Technical Conference, October, 1983, pp.82-93.
11. Guynn, E.G., and O'Brien, T.K., "The Influence of Lay-up and Thickness on Composite Impact Damage and Compression Strength," AIAA-85-0646, in Proceedings of the 26th AIAA/ASME/ASCE/AHS Structures, Structural Dynamics, and Materials Conference, Orlando, FL., April, 1985, pp.187-196.
12. Masters, J.E., "Characterization of Impact Damage Development in Graphite/Epoxy Laminates," in Fractography of Modern Engineering Materials, ASTM STP 948, 1987, pp. 238-258.
13. Bishop, S.M., and Dorey, G., "The Effect of Damage on the Tensile and Compressive Performance of Carbon Fiber Laminates," in Characterization, Analysis, and Significance of Defects in Composite Materials, AGARD CP-355, April, 1983.
14. Simonds, R.A., Bakis, C.E., and Stinchcomb, W.W., "Effects of Matrix Toughness on Fatigue Response of Graphite Fiber Composite Laminates," Presented at the 2nd ASTM Symposium on Composite Materials: Fatigue and Fracture, Cincinnati, Ohio, April, 1987.
15. O'Brien, T.K., and Raju, I.S., "Strain Energy Release Rate Analysis of Delamination Around an Open Hole in a Composite Laminate," AIAA-84-0961, Proceedings of the 25th AIAA/ASME/ASCE/AHS Structures, Structural Dynamics, and Materials Conference, Palm Springs, CA, May 1984.

16. O'Brien, T.K., "Delamination Durability of Composite Materials for Rotorcraft," Presented at the 1987 NASA/Army Rotorcraft Technology Conference, March 1987, Moffett Field, CA, (Proceedings, to be published as NASA CP, 1987).
17. Wilkins, D.J., Eisenmann, J.R., Camin, R.A., Margolis, W.S., and Benson, R.A., "Characterizing Delamination Growth in Graphite-Epoxy," in Damage in Composite Materials, ASTM STP 775, June, 1982, p. 168.
18. Mall, S., Yun, K.T., and Kochhar, N.K., "Characterization of Matrix Toughness Effects on Cyclic Delamination Growth in Graphite Fiber Composites," Presented at the 2nd ASTM Symposium on Composite Materials: Fatigue and Fracture, Cincinnati, Ohio, April, 1987.
19. Russell, A.J., and Street, K.N., "Predicting Interlaminar Fatigue Crack Growth Rates in Compressively Loaded Laminates," Presented at the 2nd ASTM Symposium on Composite Materials: Fatigue and Fracture, Cincinnati, Ohio, April, 1987.
20. Gustafson, C.G., and Hojo, M., "Delamination Fatigue Crack Growth in Unidirectional Graphite/Epoxy Laminates," *J. Reinforced Plastics*, Vol.6, No.1, January, 1987, pp. 36-52.
21. O'Brien, T.K., "Generic Aspects of Delamination in Fatigue of Composite Materials," *Journal of the American Helicopter Society*, Vol. 32, No. 1, January, 1987, pp. 13-18.
22. Martin, R.H., and Murri, G.B., "Characterization of Mode I and Mode II Delamination Growth and Thresholds in Graphite/PEEK Composites," to be presented at the 9th ASTM Symposium on Composite Materials: Testing and Design, Reno, Nevada, April, 1988.

23. O'Brien, T.K.: Characterization of Delamination Onset and Growth in a Composite Laminate. Damage in Composite Materials, ASTM STP 755, 1982. pp. 140-167.
24. Russell, A.J. and Street, K.N., "Moisture and Temperature Effects on the Mixed-Mode Delamination Fracture of Unidirectional Graphite/Epoxy," in Delamination and Debonding of materials, ASTM STP 876, Oct, 1985, pp. 349-370.
25. Poursartip, A., "The Characterization of Edge Delamination Growth in Composite Laminates Under Fatigue Loading," in Toughened Composites, ASTM STP 937, pp.222-241.
26. O'Brien, T.K.: Mixed-Mode Strain Energy Release Rate Effects on Edge Delamination of Composites. Effects of Defects in Composite Materials, ASTM STP 836, 1984, pp. 125-142.
27. O'Brien, T.K., "Tension Fatigue Behavior of Quasi-Isotropic Graphite/Epoxy Laminates," in Fatigue and Creep of Composite Materials, Proceedings of the 3rd Riso International Symposium on Metallurgy and Materials Science, Riso National Laboratory, Roskilde, Denmark, 1982, pp. 259-264.
28. O'Brien, T.K., "Fatigue Delamination Behavior of PEEK Thermoplastic Composite Laminates," in Proceedings of the American Society for Composites First Technical Conference, Dayton, Ohio, Oct. 1986. Technomic Publishing Co., Lancaster, PA, Oct. 1986, pp. 404-420.
29. O'Brien, T.K., Murri, G.B., and Salpekar, S.A., "Interlaminar Shear Fracture Toughness and Fatigue Thresholds for Composite Materials," NASA TM 89157, August 1987, (Presented at the 2nd ASTM Symposium on Composite Materials: Fatigue and Fracture, Cincinnati, Ohio, April, 1987.)
30. Adams, D.F., Zimmerman, R.S., and Odem, E.M., "Frequency and Load Ratio Effects on Critical Strain Energy Release Rate  $G_c$  Thresholds of Graphite Epoxy Composites," in Toughened Composites, ASTM STP 937, 1987, p.242.

31. O'Brien, T.K., Zanotti, C., and Rigamonti, M., "Tension Fatigue Life Analysis for Composite Laminates," NASA TM 100549, 1988.
32. O'Brien, T.K., "Analysis of Local Delaminations and Their Influence on Composite Laminate Behavior," in Delamination and Debonding of Materials, ASTM STP 876, 1985, pp. 282-297.
33. Caslini, M., Zanotti, C., and O'Brien, T.K., "Fracture Mechanics of Matrix Cracking and Delamination in Glass Epoxy Laminates," NASA TM 89007, Sept. 1986.
34. O'Brien, T.K.; Crossman, F.W.; and Ryder, J.R.: Stiffness, Strength, and Fatigue Life Relationships for Composite Laminates, Dayton, Ohio, 1981, Proceedings of the Seventh Annual Mechanics of Composites Review, AFWAL-TR-82-4007, April 1982, pp. 79-90.
35. O'Brien, T.K., "The Effect of Delamination on the Tensile Strength of Unnotched, Quasi-Isotropic, Graphite Epoxy Laminates," Proceedings of the SESA/JSME Joint Conference on Experimental Mechanics, Honolulu, Hawaii, May, 1982, Part I, SESA, Brookfield Center, CT, pp. 236-243.
36. Ryder, J.T., and Crossman, F.W., "A Study of Stiffness, Residual Strength, and Fatigue Life Relationships for Composite Laminates," NASA CR-172211, Oct. 1983.
37. Jamison, R.D., Schulte, K., Reifsnider, K.L., and Stinchcomb, W.W., "Characterization and Analysis of Damage Mechanisms in Tension-Tension Fatigue of Graphite/Epoxy Laminates," in Effects of Defects in Composite Materials, ASTM STP 836, 1984, pp.21-55.
38. O'Brien, T.K., "Characterizing Delamination Resistance of Toughened Resin Composites," in Tough Composites, NASA CP 2334, 1984.
39. O'Brien, T.K.; Johnston, N.J.; Morris, D.H., and Simonds, R.A., "Determination of Interlaminar Fracture Toughness and Fracture Mode

- Dependence of Composites Using the Edge Delamination Test," in Testing, Evaluation, and Quality Control of Composites, Butterworth Scientific Ltd., Kent, England, 1983.
40. Aliyu, A.A., and Daniel, I.M., "Effects of Strain Rate on Delamination Fracture Toughness of Graphite/Epoxy," in Delamination and Debonding of Materials, ASTM STP 876, 1985, pp.336-348.
  41. Daniel, I.M., Shareef, I., and Aliyu, A.A., "Rate Effects on Delamination Fracture Toughness of a Toughened Graphite/Epoxy," in Toughened Composites, ASTM STP 937, pp.260-274.
  42. McCarty, J.E., and Ratwani, M.M., "Damage Tolerance of Composites," Interim Report No.3, AFWAL Contract F33615-82-C-3213, Boeing Military Airplane Co., March, 1984.
  43. Lubowinski, S.J., and Poe, C.C., "Fatigue Characterization of Stitched Graphite Epoxy Composites," Proceedings of the FIBER-TEX 87 Conference, Greenville, SC, Nov. 1987, to be Published as a NASA CP, 1988.
  44. Bakis, C.E., and Stinchcomb, W.W., "Response of Thick, Notched Laminates Subjected to Tension-Compression Cyclic Loads," in Composite Materials: Fatigue and Fracture, ASTM STP 907, June, 1986, pp.314-334.
  45. Chai, H., Babcock, C.D., and Knauss, W.G., "One-Dimensional Modeling of Failure in Laminated Plates by Delamination Buckling," Int. J. of Solids and Structures, Vol. 17, No.11, pp.1069-1083.
  46. Whitcomb, J.D., "Finite Element Analysis of Instability-Related Delamination Growth," J. of Composite Materials, Vol.15, 1981, pp.403-426.
  47. Chai, H., and Babcock, C.D., "Two-Dimensional Modeling of Compressive Failure in Delaminated Laminates," J. of Composite Materials, Vol. 19, Jan. 1985, pp.67-98.

48. Flanagan, G., "2-D Delamination Growth in Composite Laminates under Compression Loading," Presented at the 8th ASTM Symposium on Composite Materials: Testing and Design, Charleston, SC, March, 1986.
49. Williams, J.F., Stouffer, D.C., Ille, S., and Jones, R., "An Analysis of Delamination Behavior," Composite Structures, Vol.5, 1986, pp.203-216.
50. Murri, G.B., and Guynn, E.G., "Analysis of Delamination Growth from Matrix Cracks in Laminates Subjected to Bending Loads," NASA TM 87754, July, 1986. (Presented at the 8th ASTM Symposium on Composite Materials: Testing and Design, Charleston, SC, March, 1986.)



ORIGINAL PAGE IS  
OF POOR QUALITY.

[45/-45/0/90]s

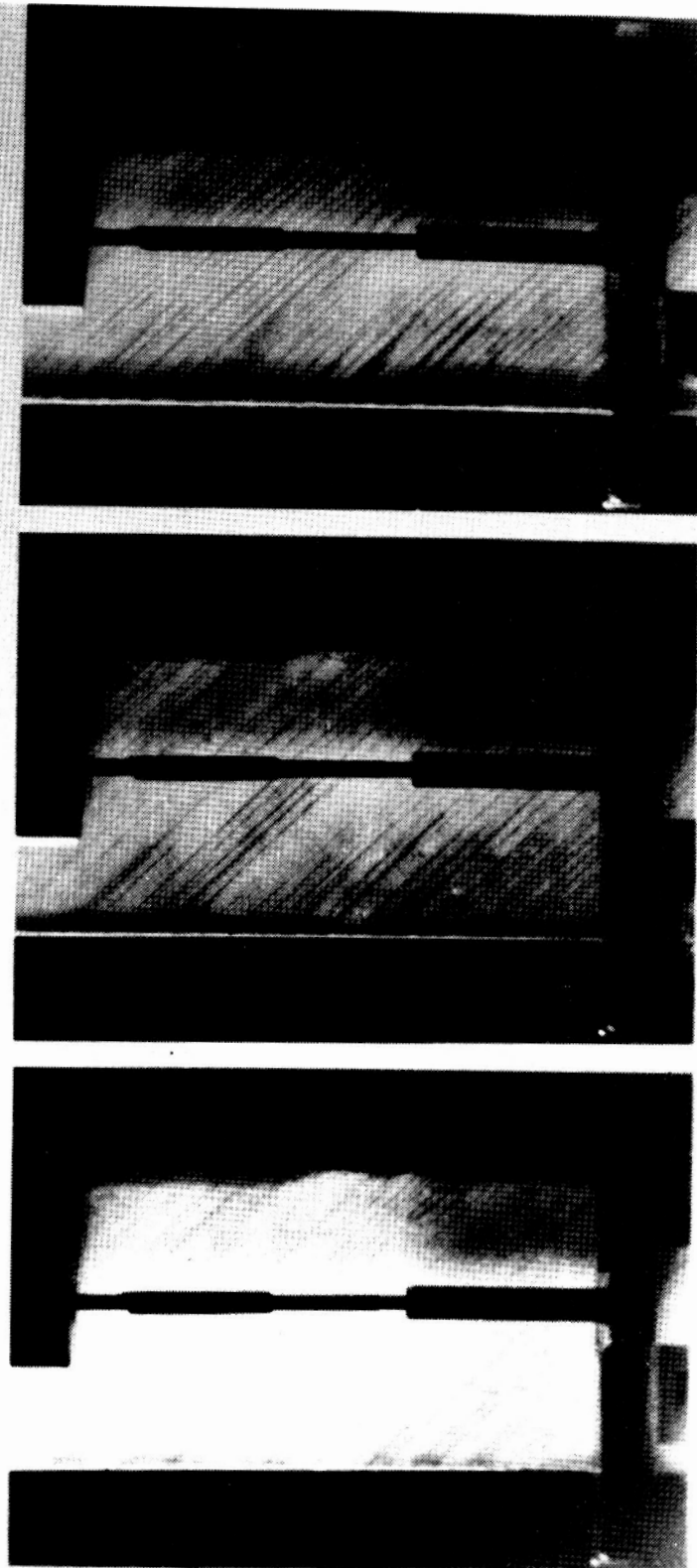


Figure 1. - Glass-epoxy tensile fatigue test.

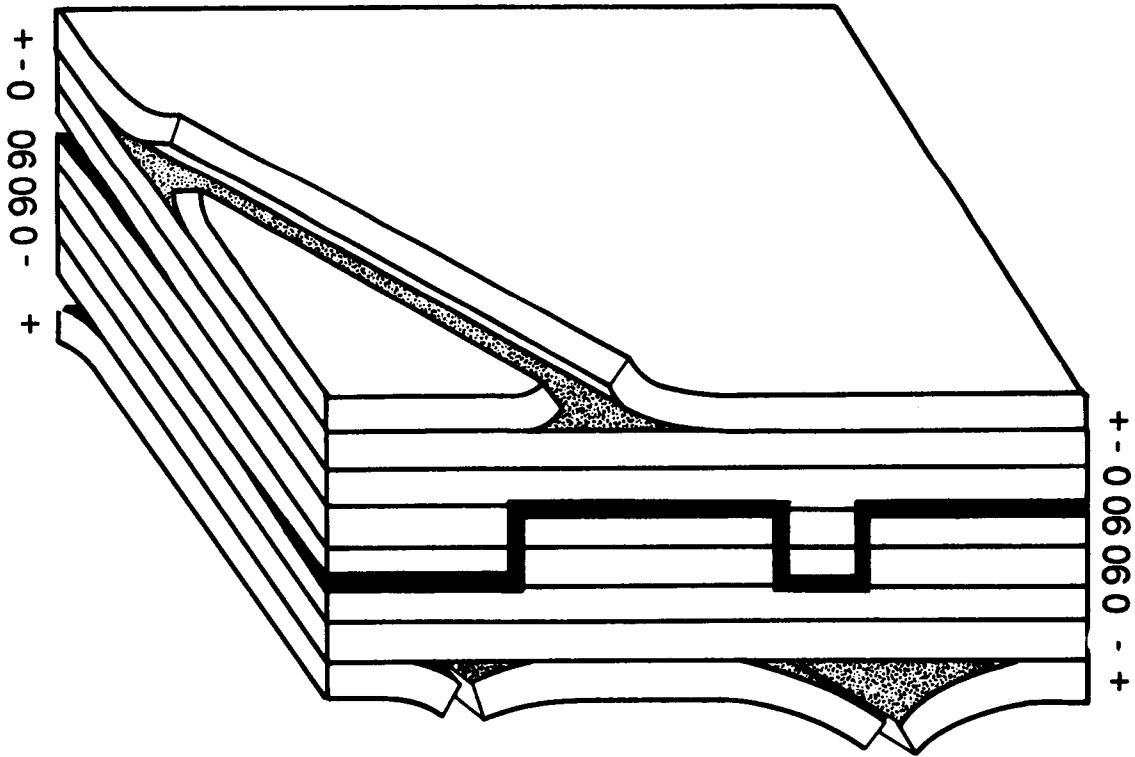


Figure 2. - Schematic of delamination in quasi-isotropic laminate subjected to cyclic tension.

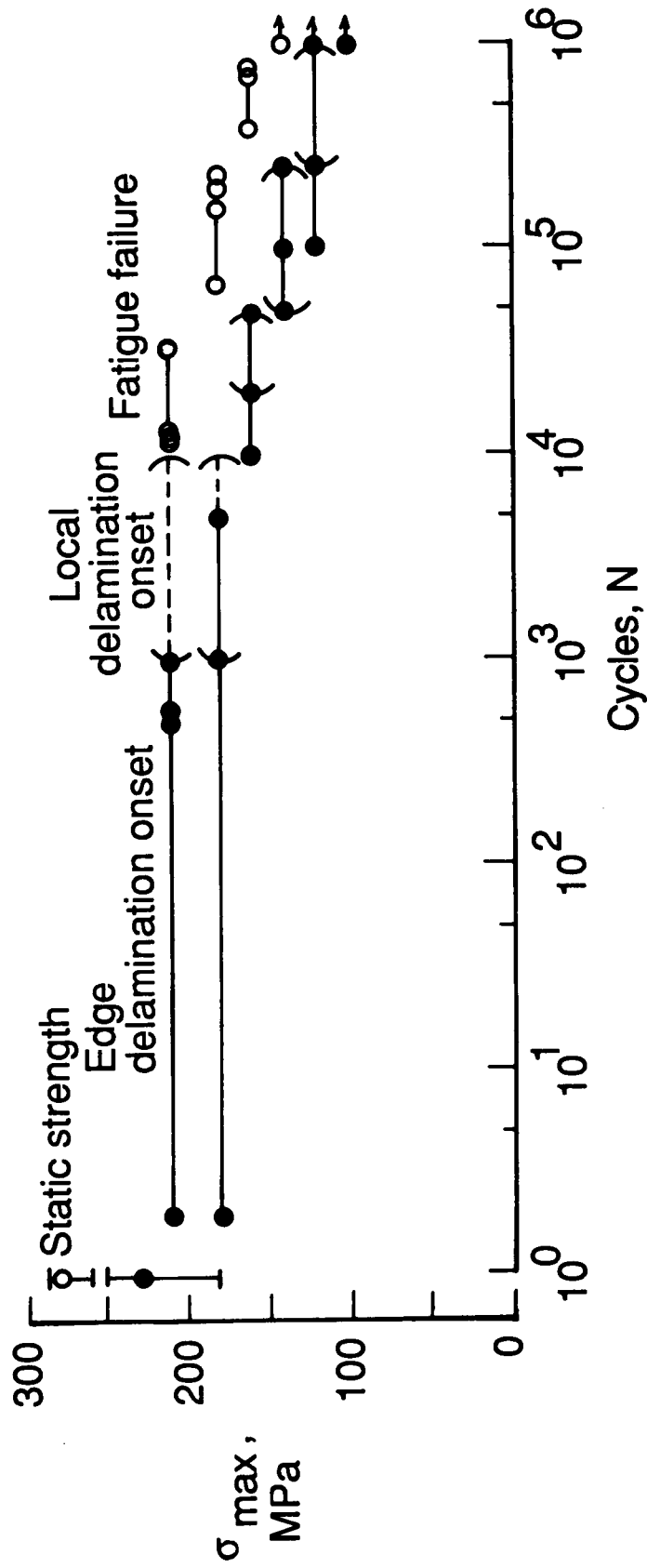


Figure 3. - Tension fatigue behavior of (45/-45/0/90)<sub>s</sub> X751/50 E-glass epoxy laminates.

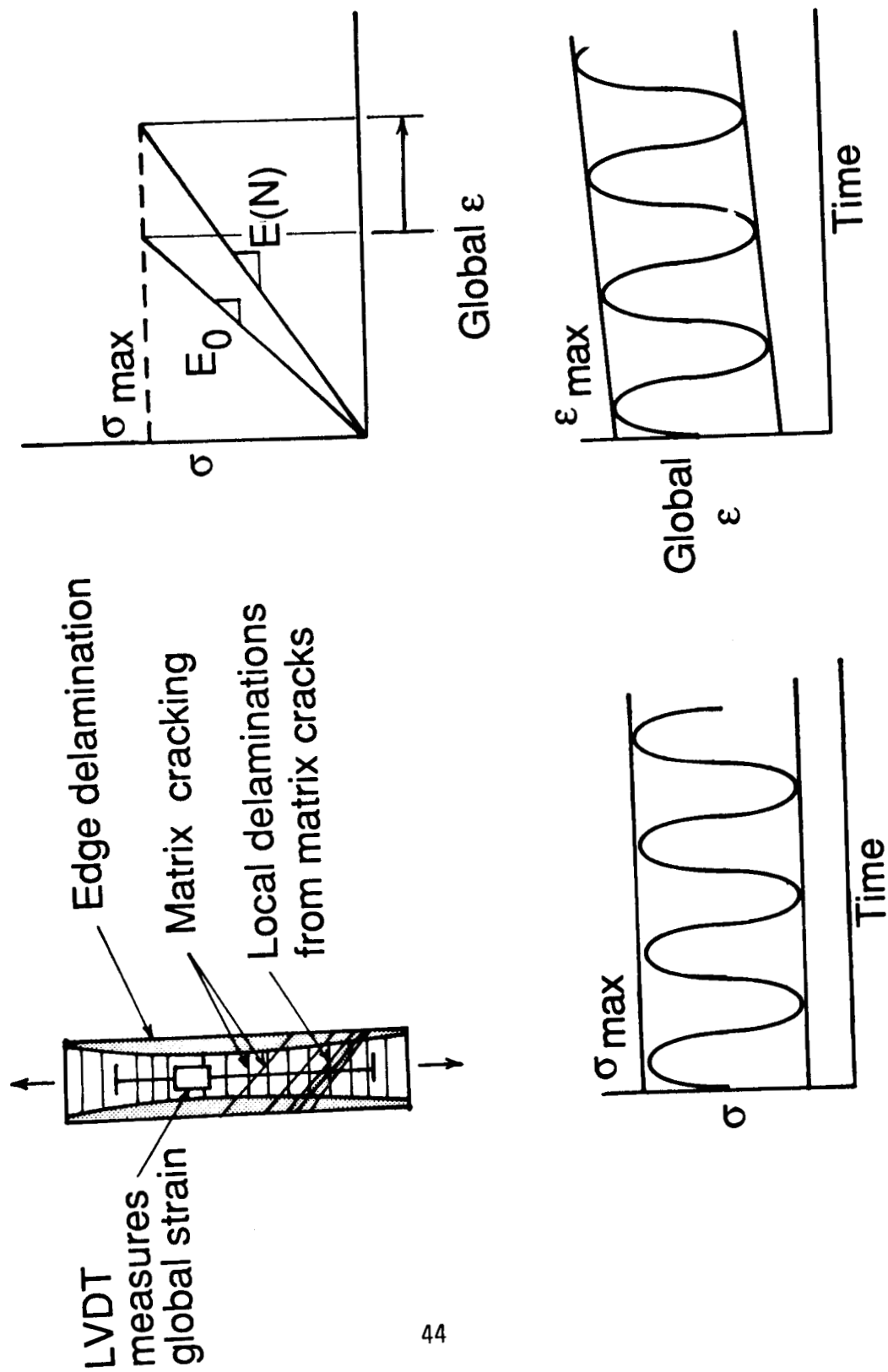


Figure 4. - Influence of damage on laminate stiffness.

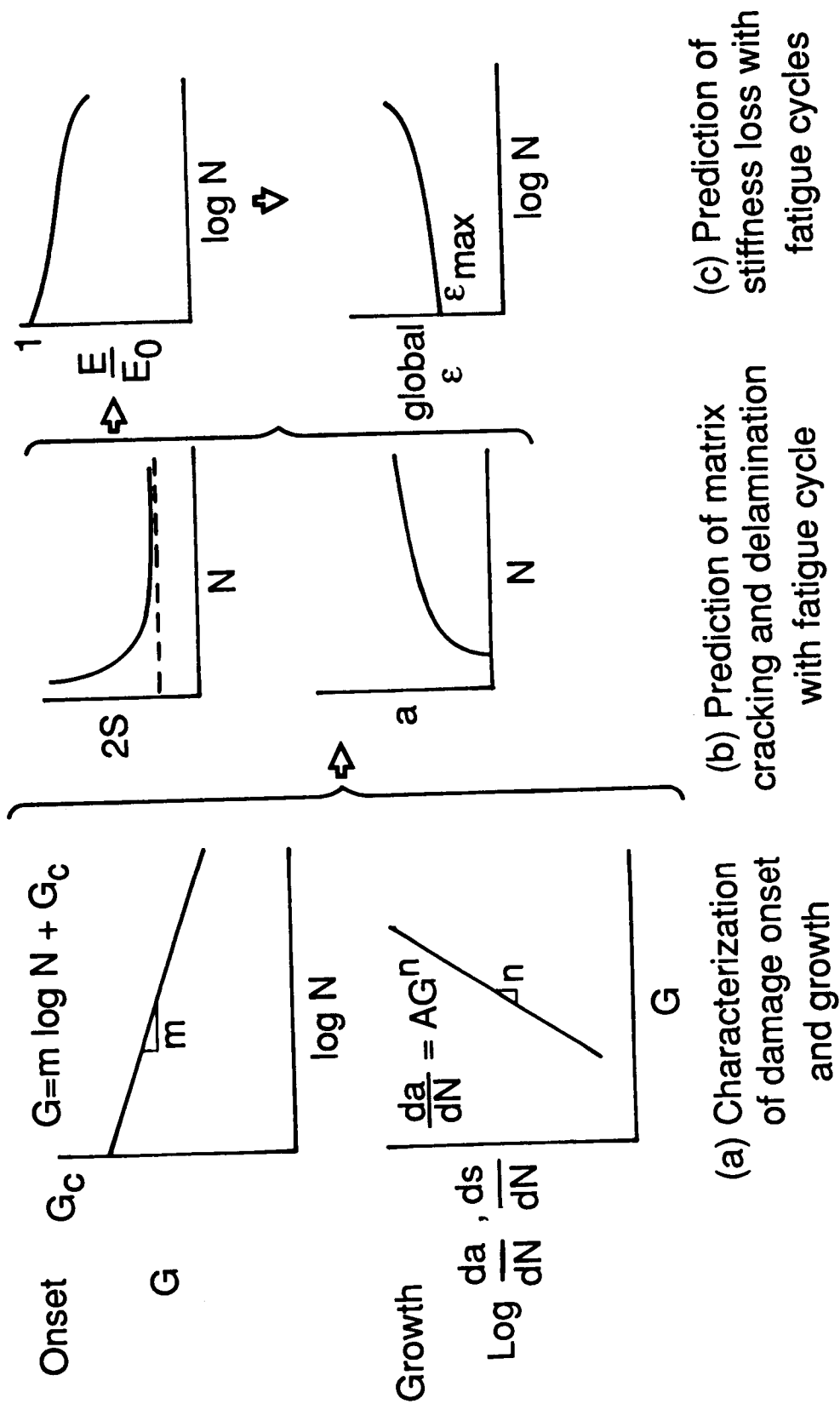


Figure 5. - Prediction of stiffness loss in composite laminates.

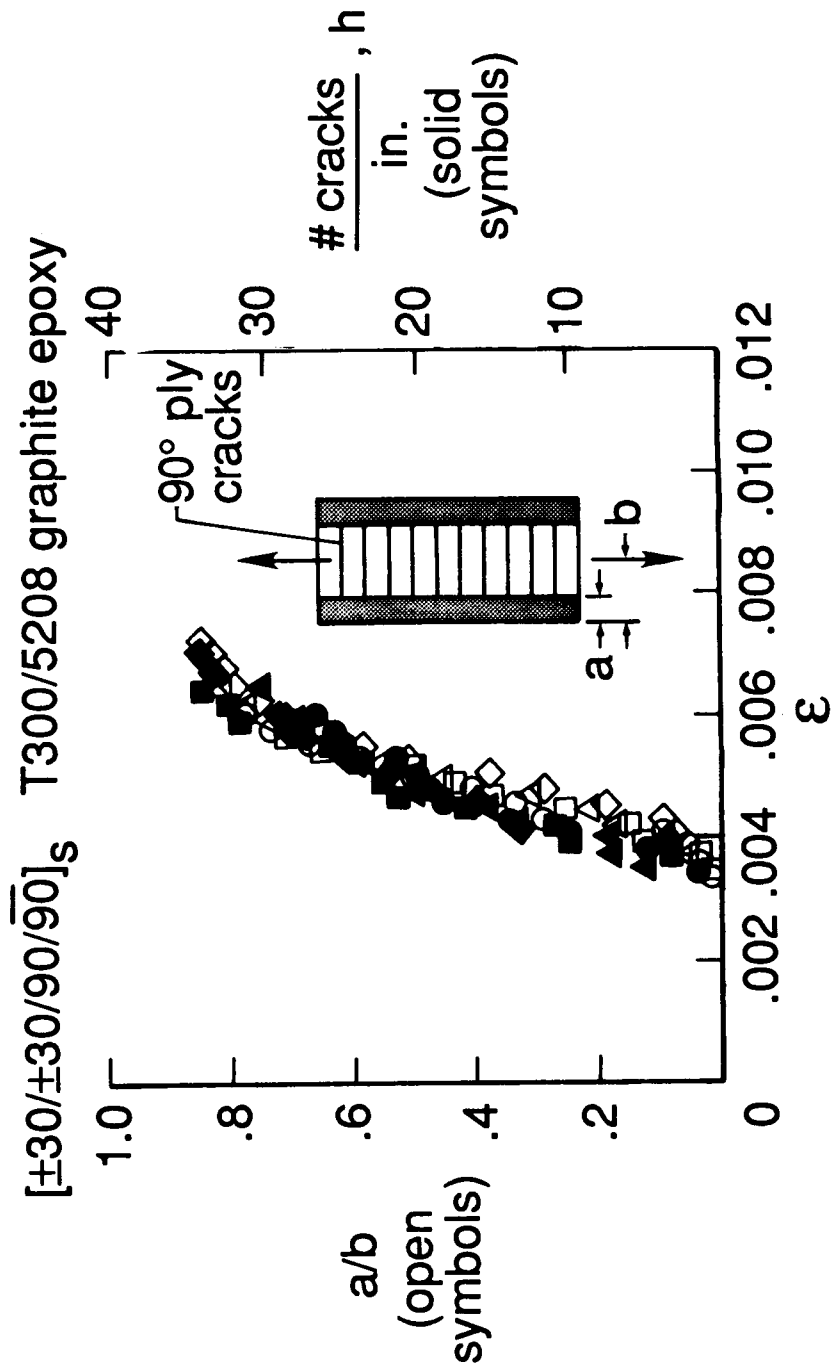


Figure 6. - Correlation of stable edge delamination growth with accumulation of 90-degree ply matrix cracks.

$\epsilon_F$  = strain at failure in static test

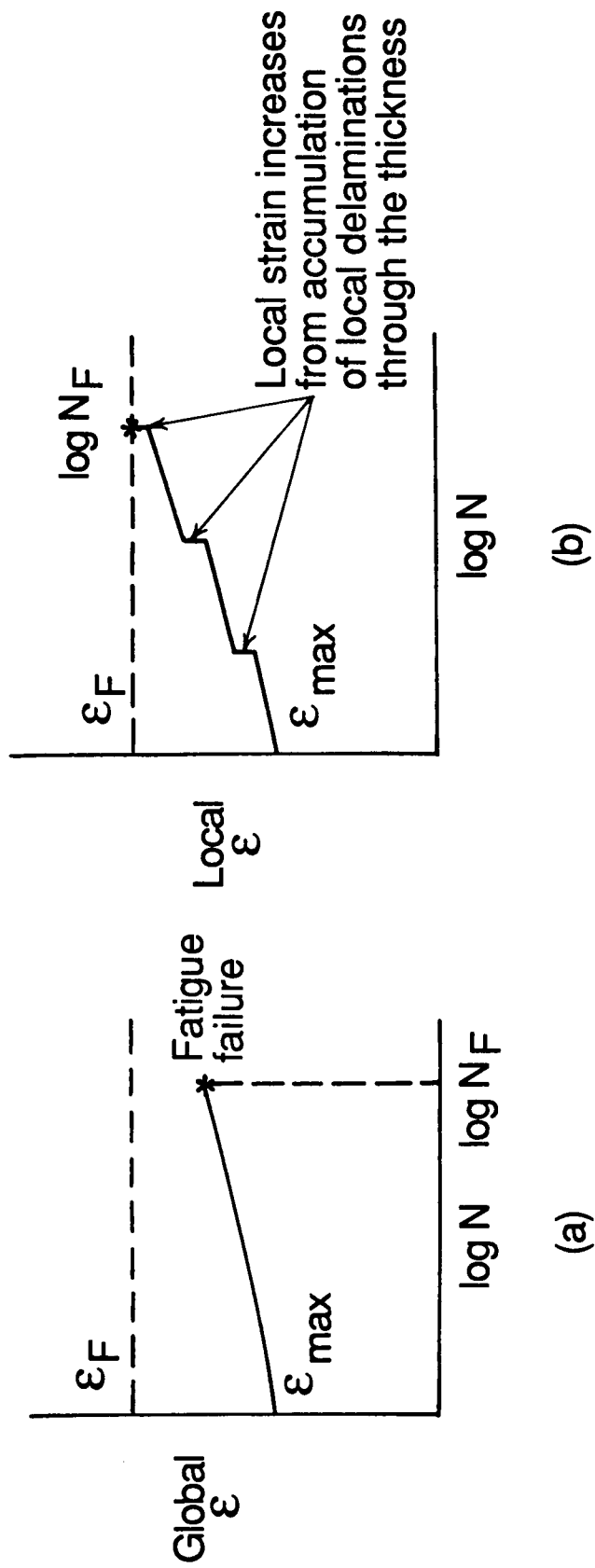
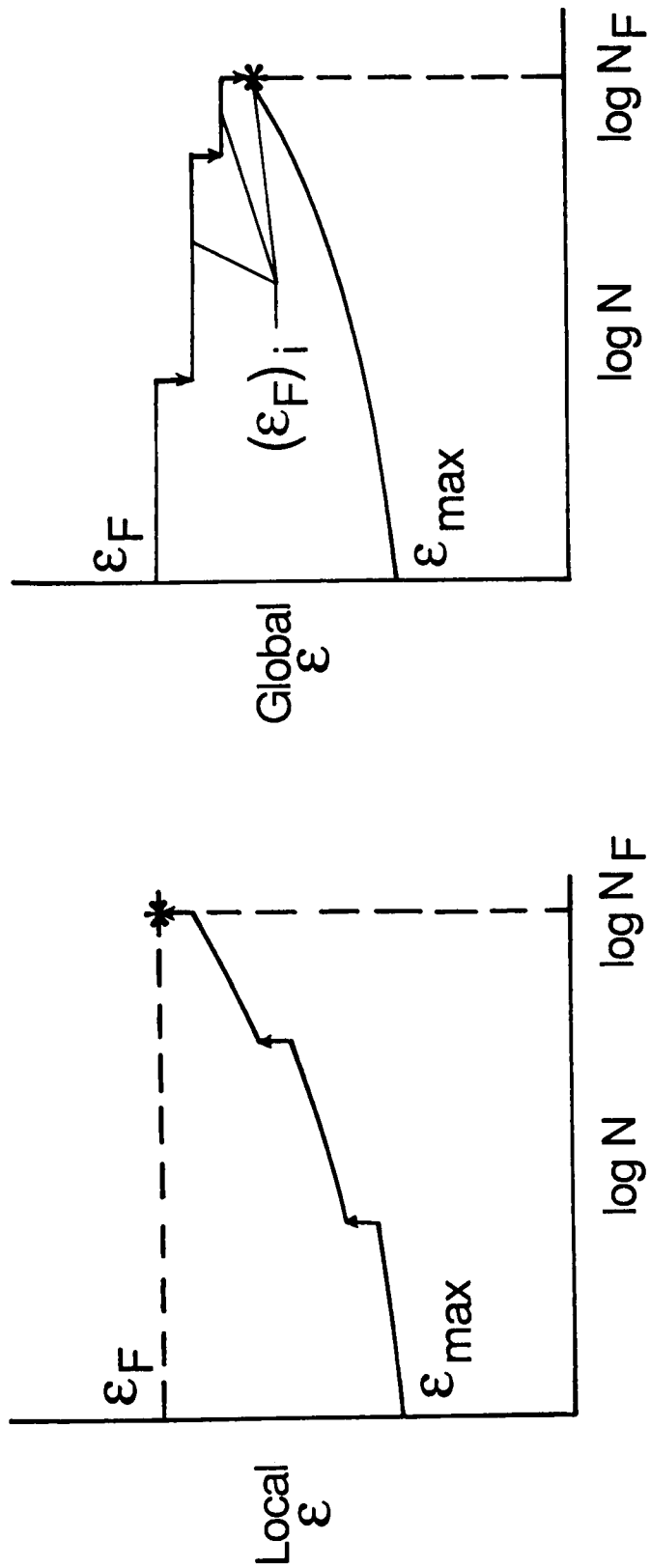


Figure 7. - Increase in global versus local strain in zero degree plies.



$$(b) (\epsilon_F)_i = \frac{\epsilon_F}{(K_\epsilon)_i}$$

$$(a) \text{ Local } \epsilon = K_\epsilon \epsilon_{MAX}$$

Figure 8. - Effective reduction in  $\epsilon_F$  due to local delamination accumulation through the laminate thickness.



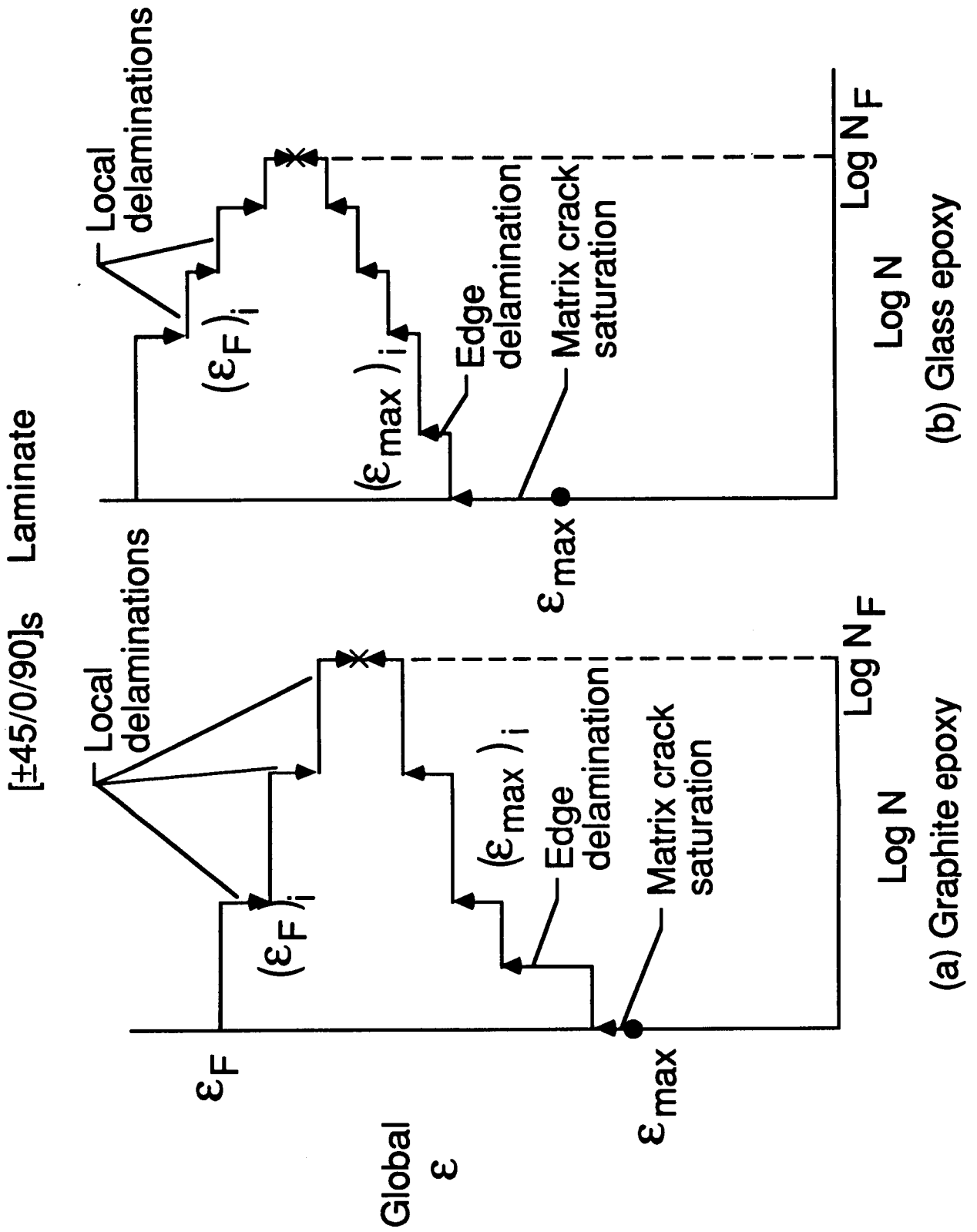


Figure 9. - Damage-threshold/fail-safety analysis.

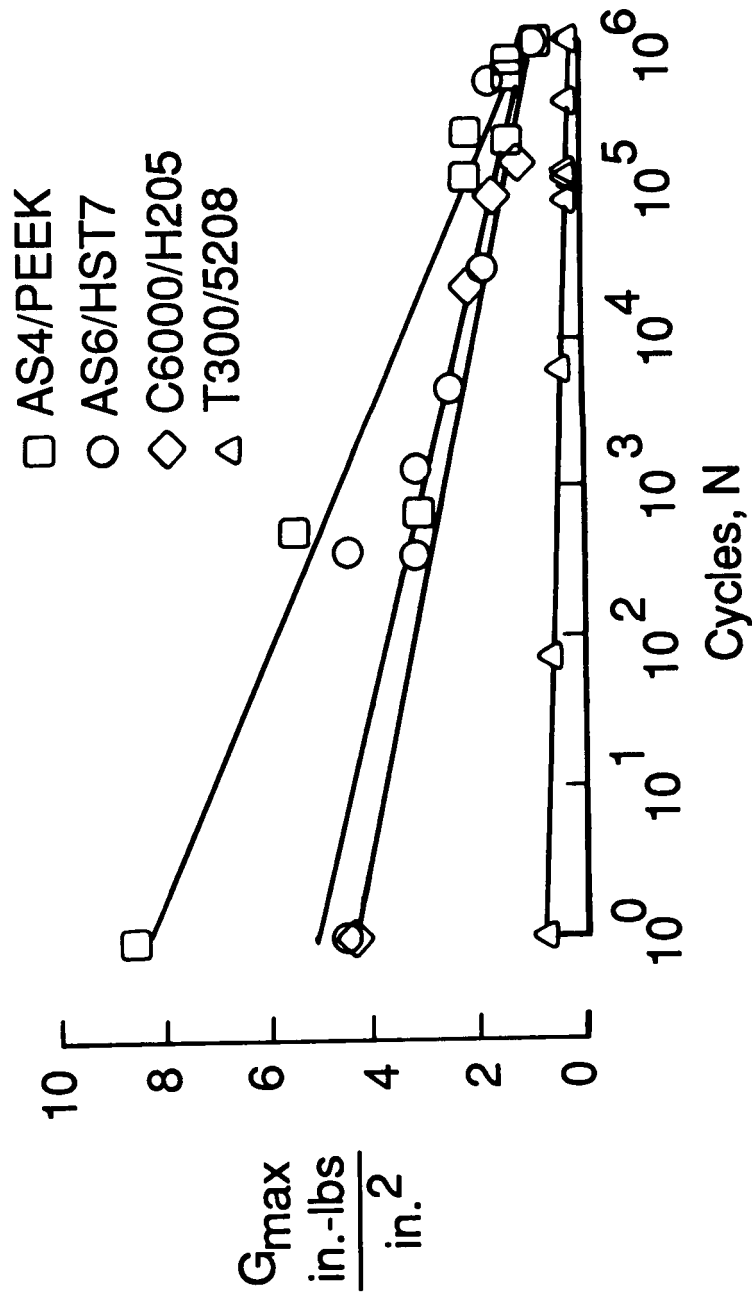


Figure 10. - Mechanical strain energy release rate at delamination onset as a function of fatigue cycles.

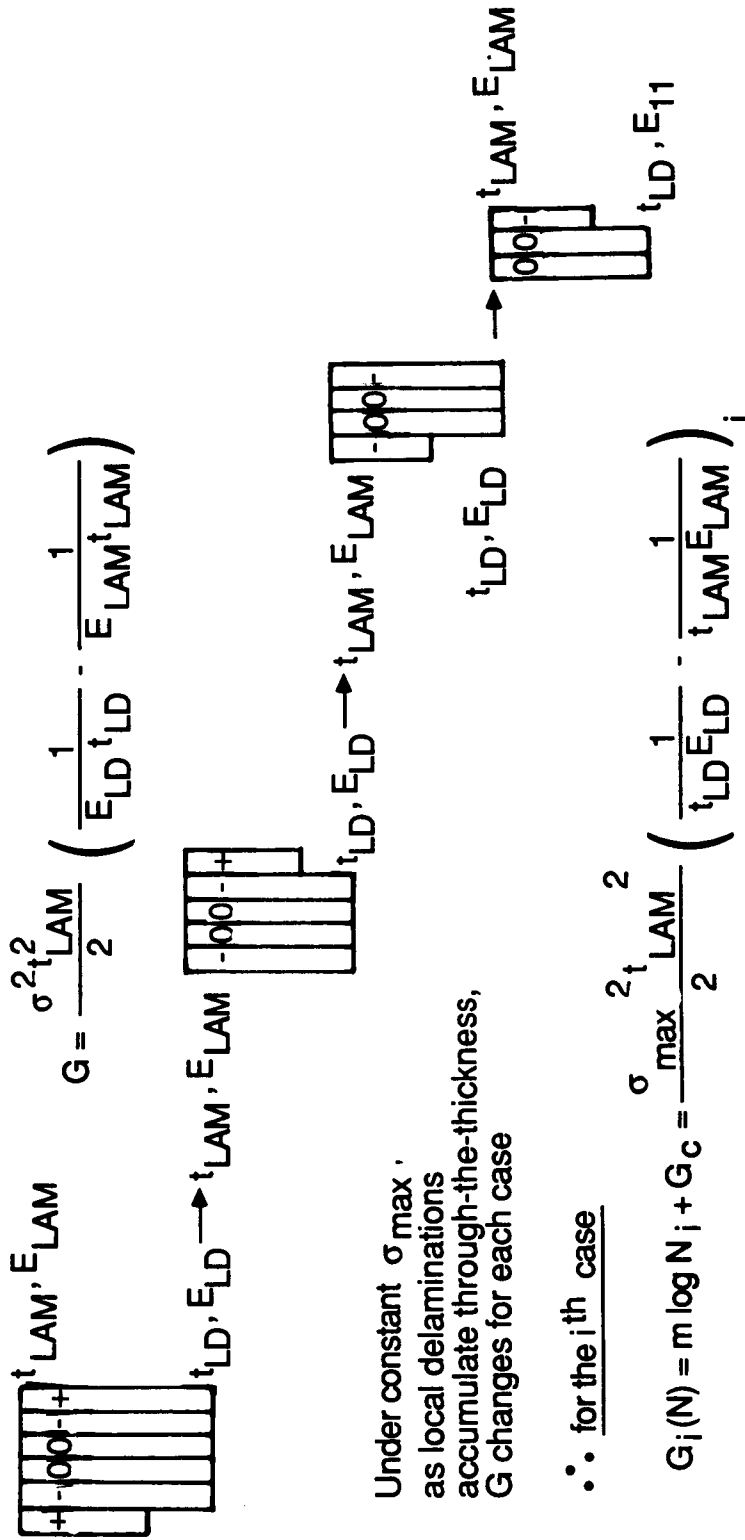


Figure 11. - Strain energy release rate for local delamination onset.

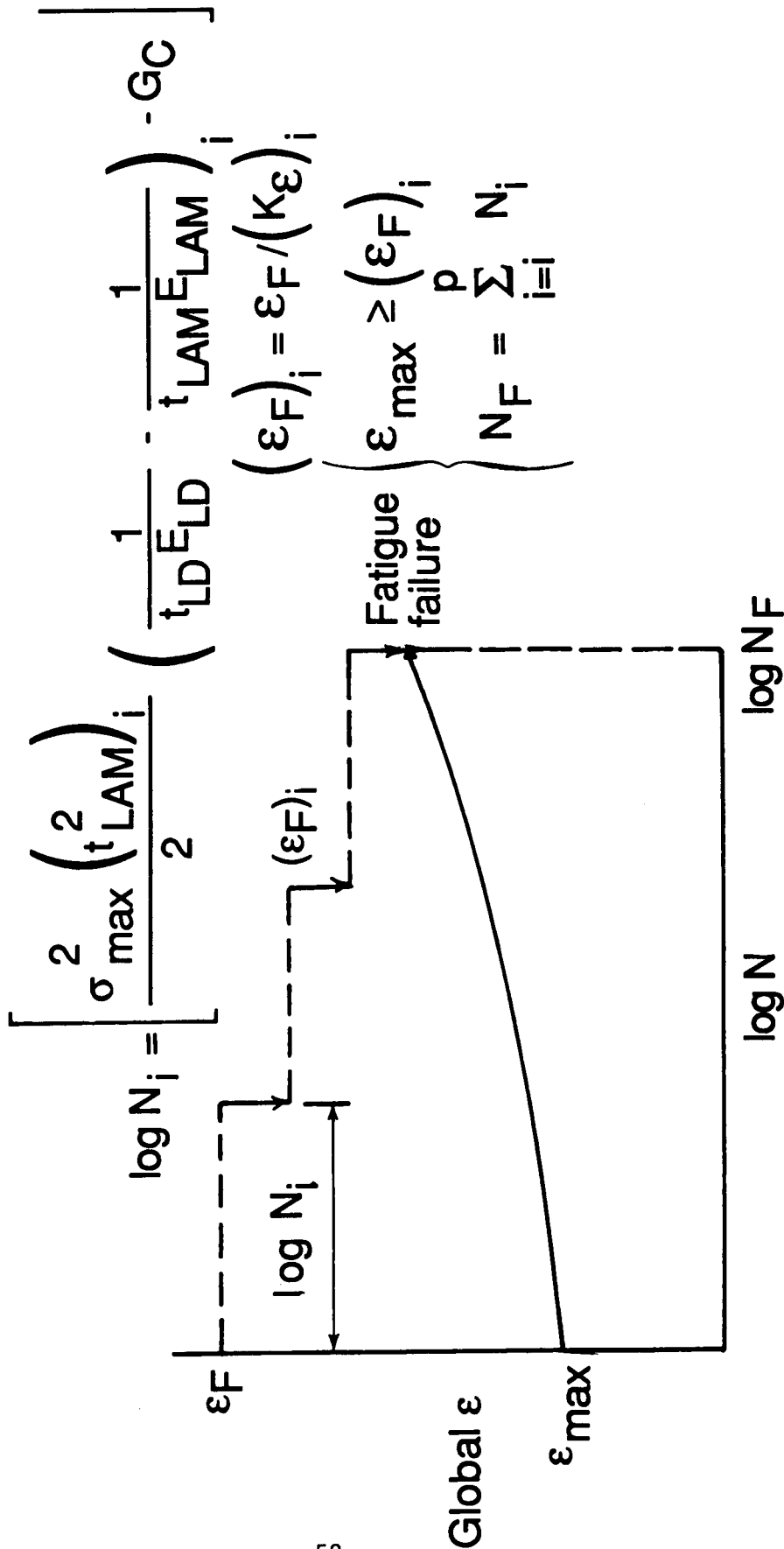


Figure 12. - Reduction in global  $\epsilon_F$  due to local delamination accumulation through the thickness.

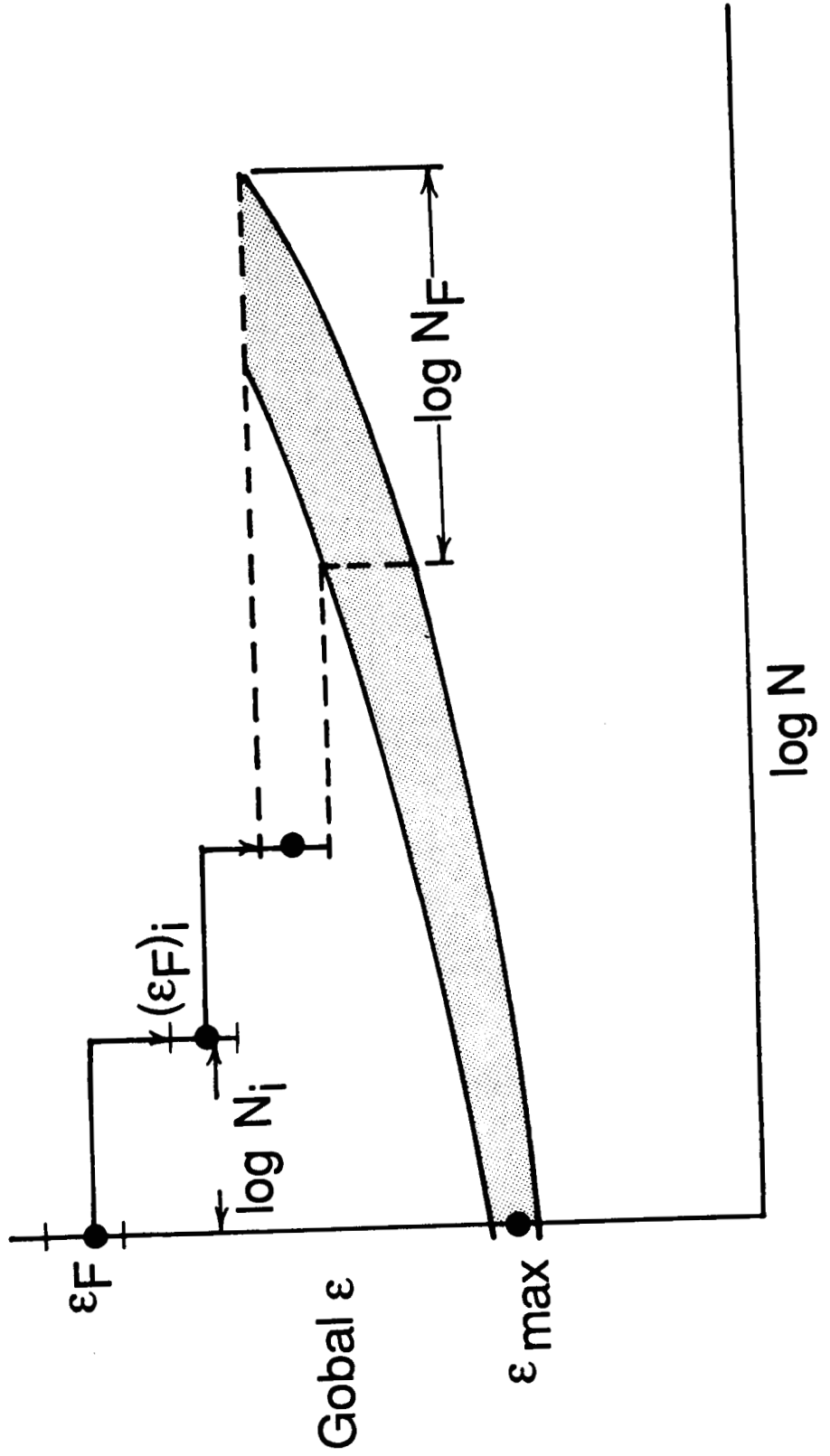


Figure 13. - Tension fatigue life prediction for composite laminates.

[±45/0/90]<sub>s</sub> E-glass epoxy x751/50

- $G_c$  for edge delamination
- Edge delamination in fatigue

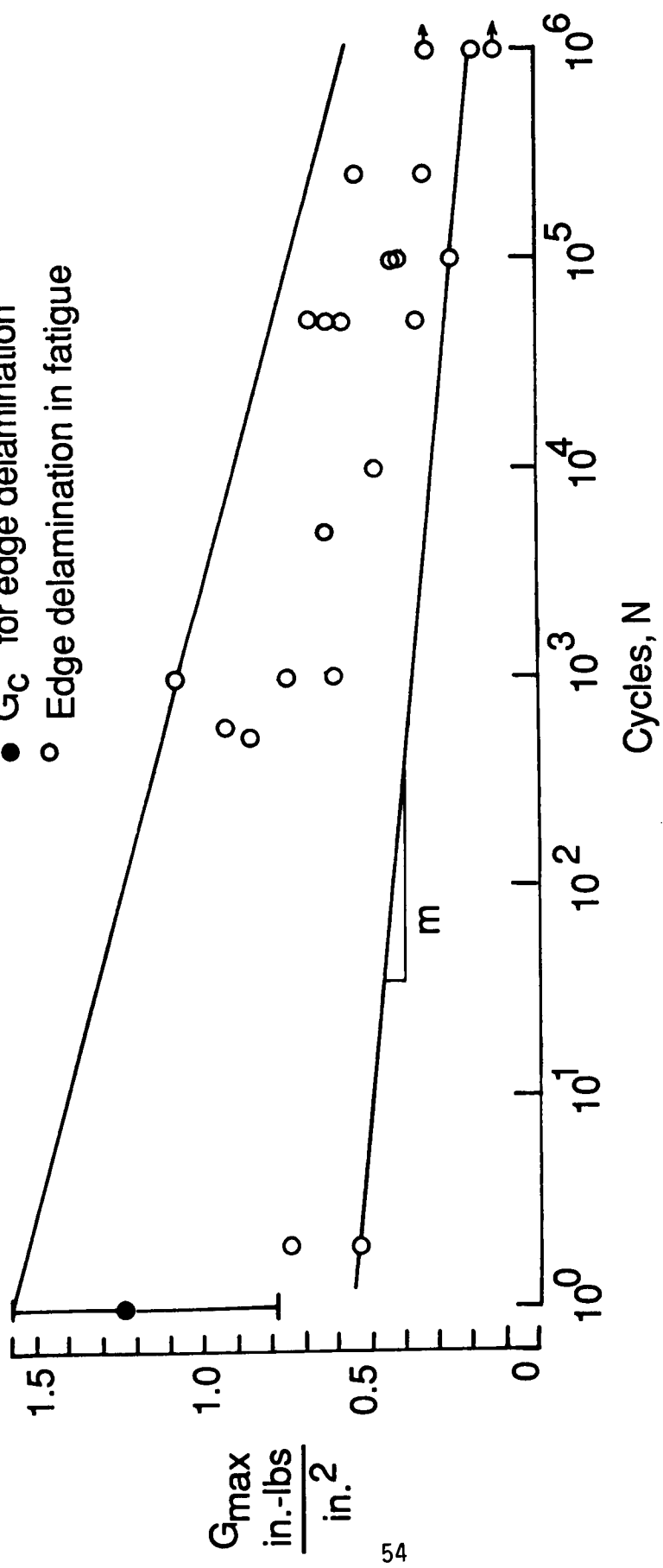


Figure 14. - Delamination onset criterion.

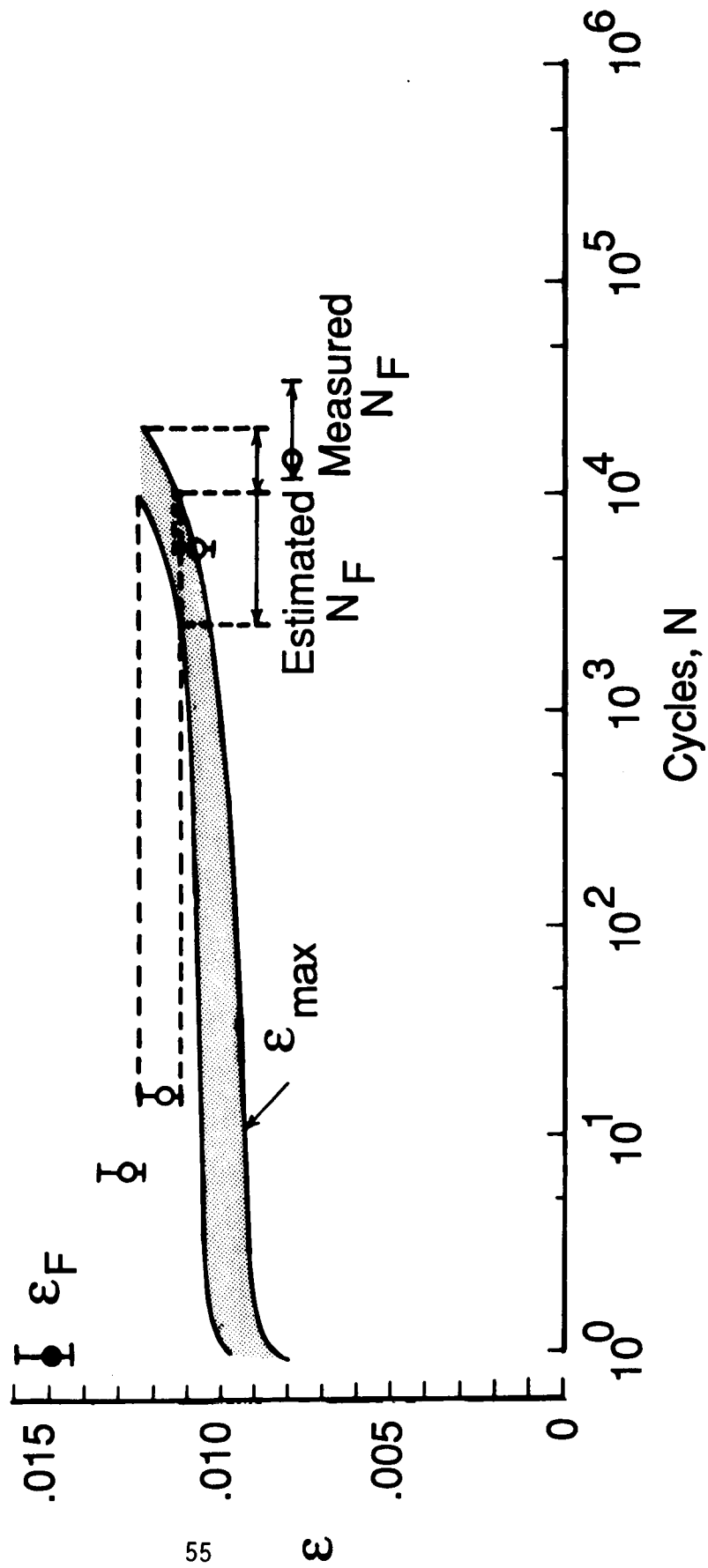


Figure 15. - Tension fatigue life estimation for (45/-45/0/90)<sub>s</sub> X751/50 E-glass epoxy.

[±45/0/90]<sub>s</sub> X751/50 E-glass Epoxy

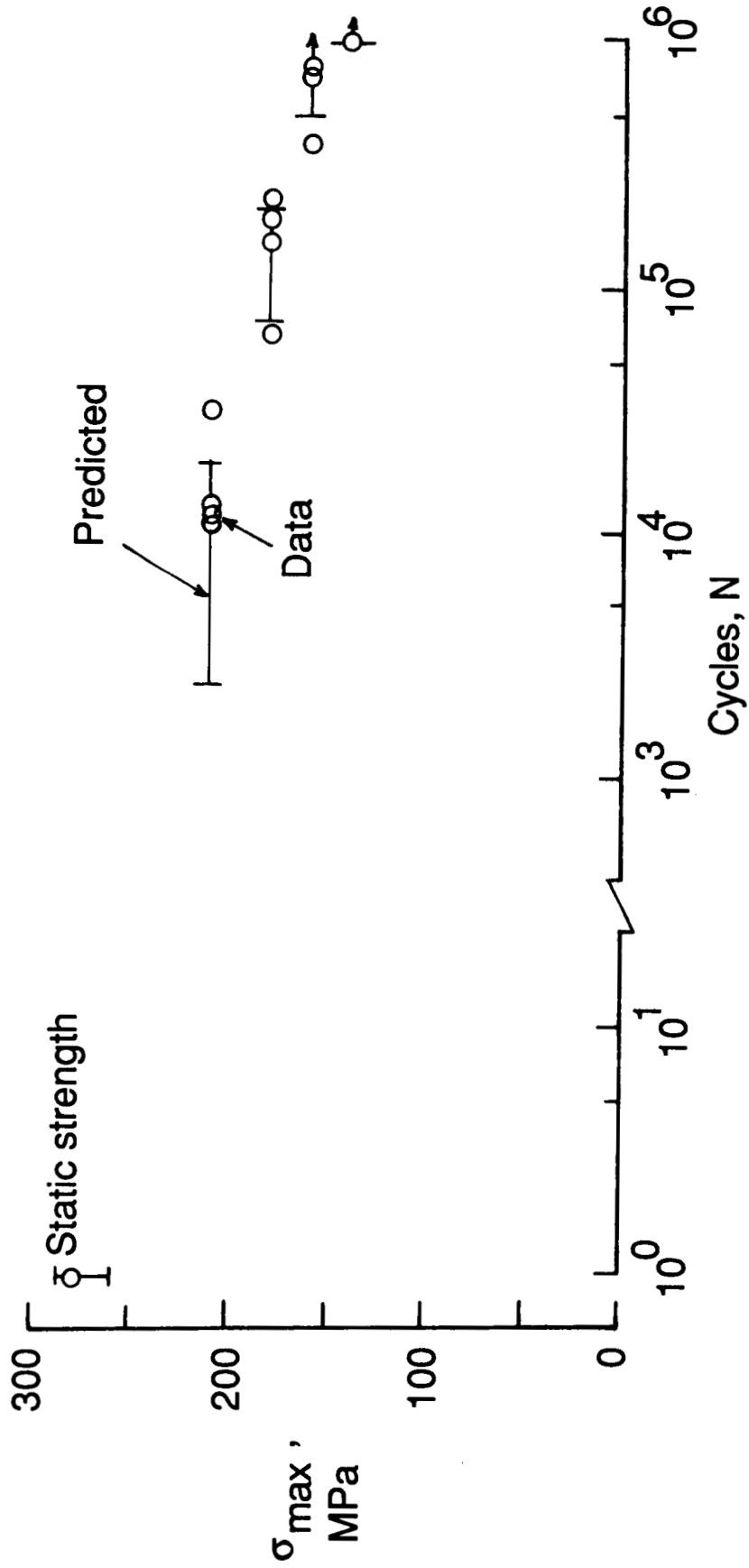


Figure 16. - Fatigue life prediction based on local delamination accumulation through the thickness.



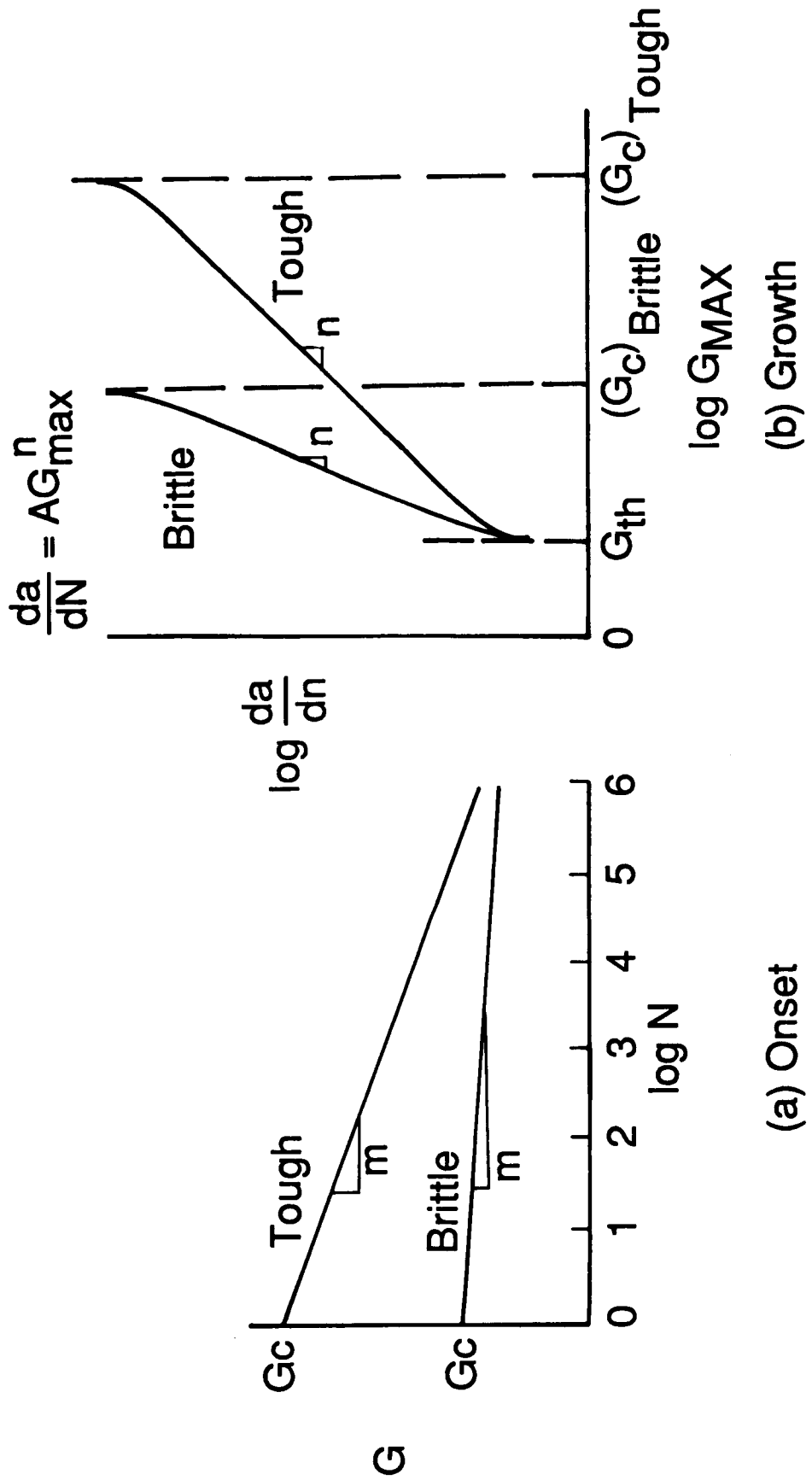


Figure 17. - Effect of matrix toughness on delamination onset and growth.

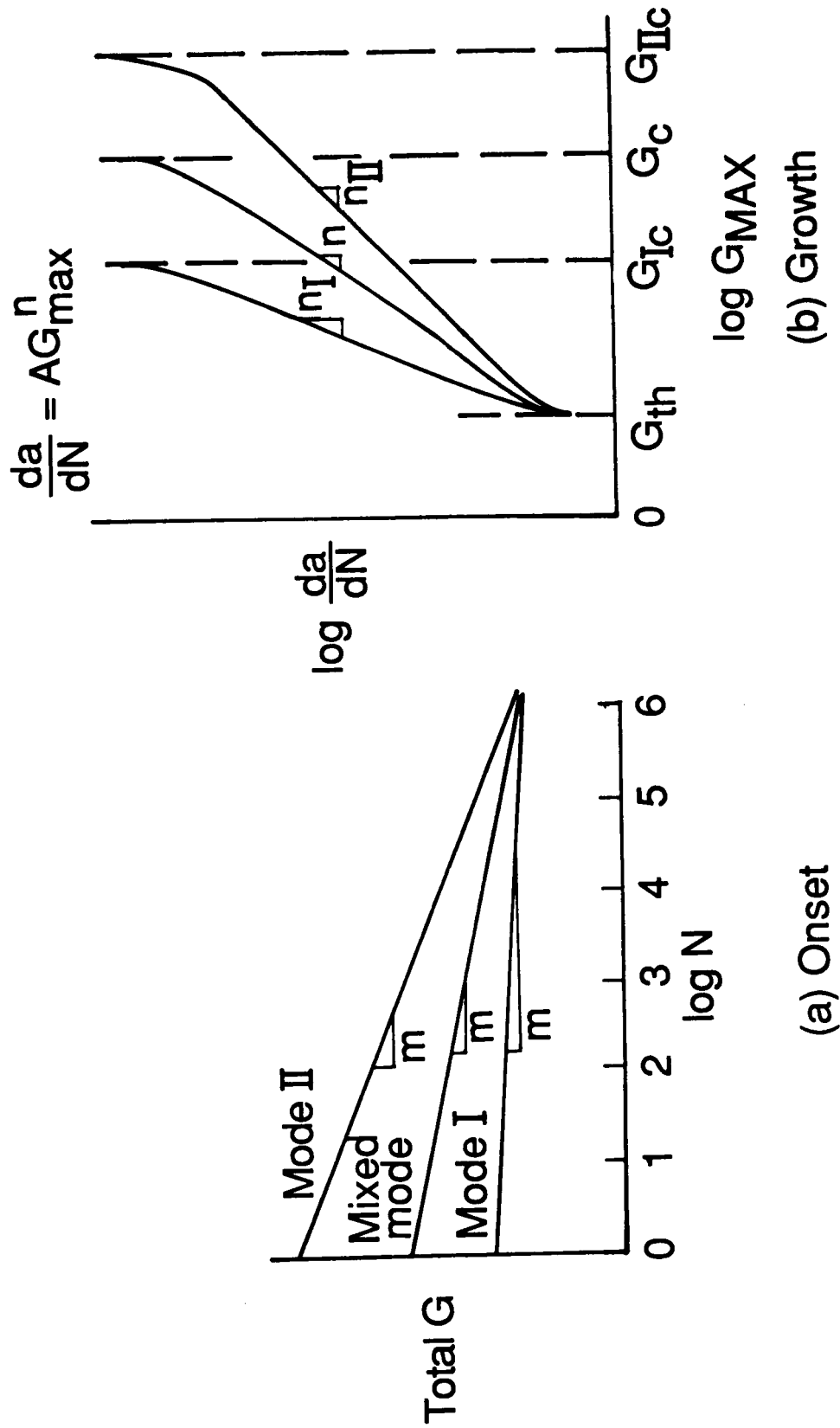
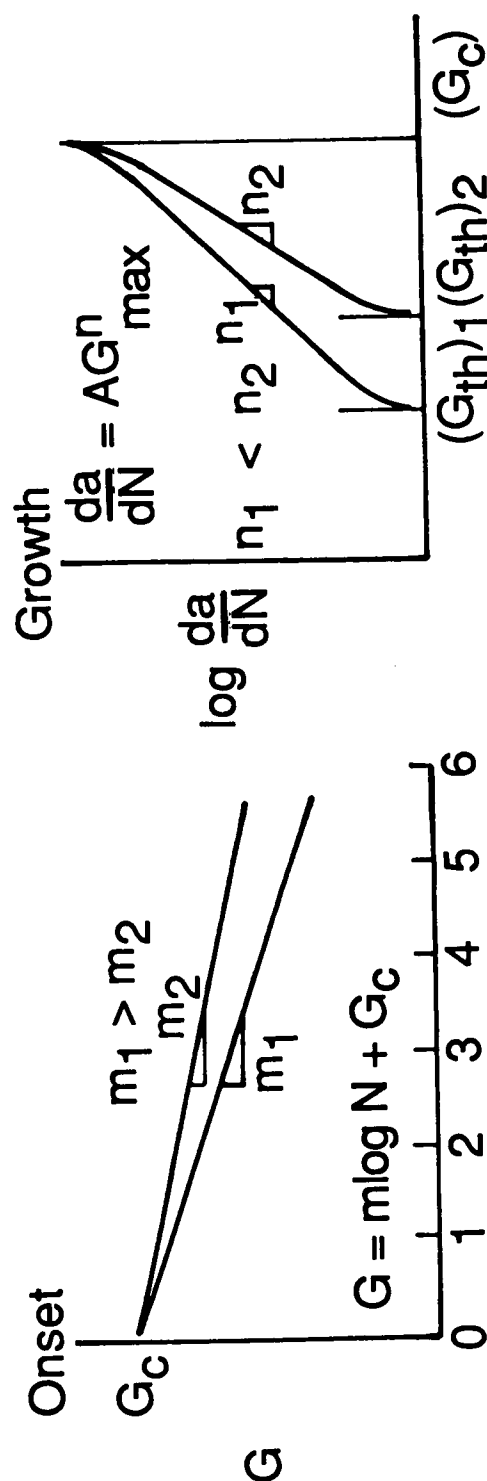
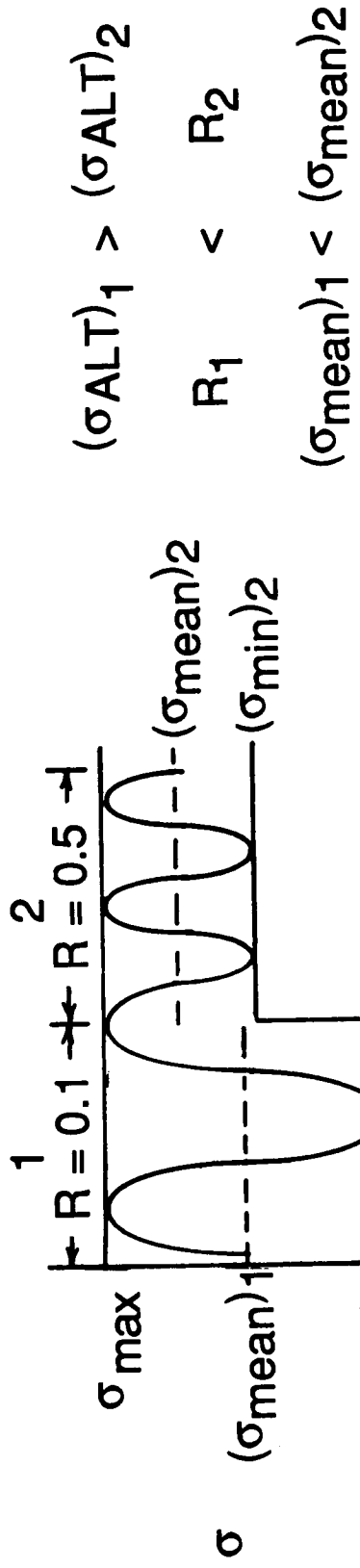


Figure 18. - Effect of mixed-mode ratio on delamination onset and growth.



(a) Onset

(b) Growth

Figure 19. - Effect of R-ratio and mean load on delamination criteria.

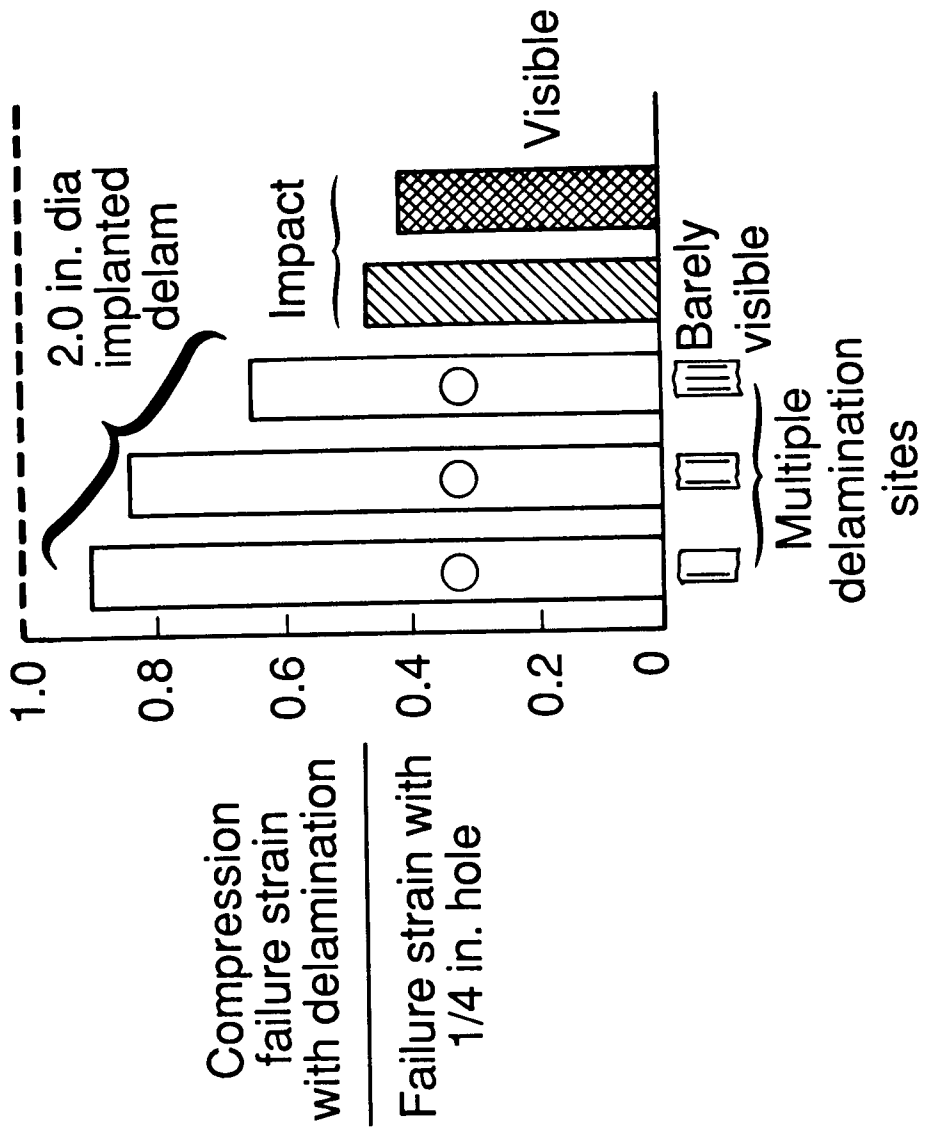


Figure 20. - Normalized compression failure strain reduction for laminates with implanted delaminations or impact damage.

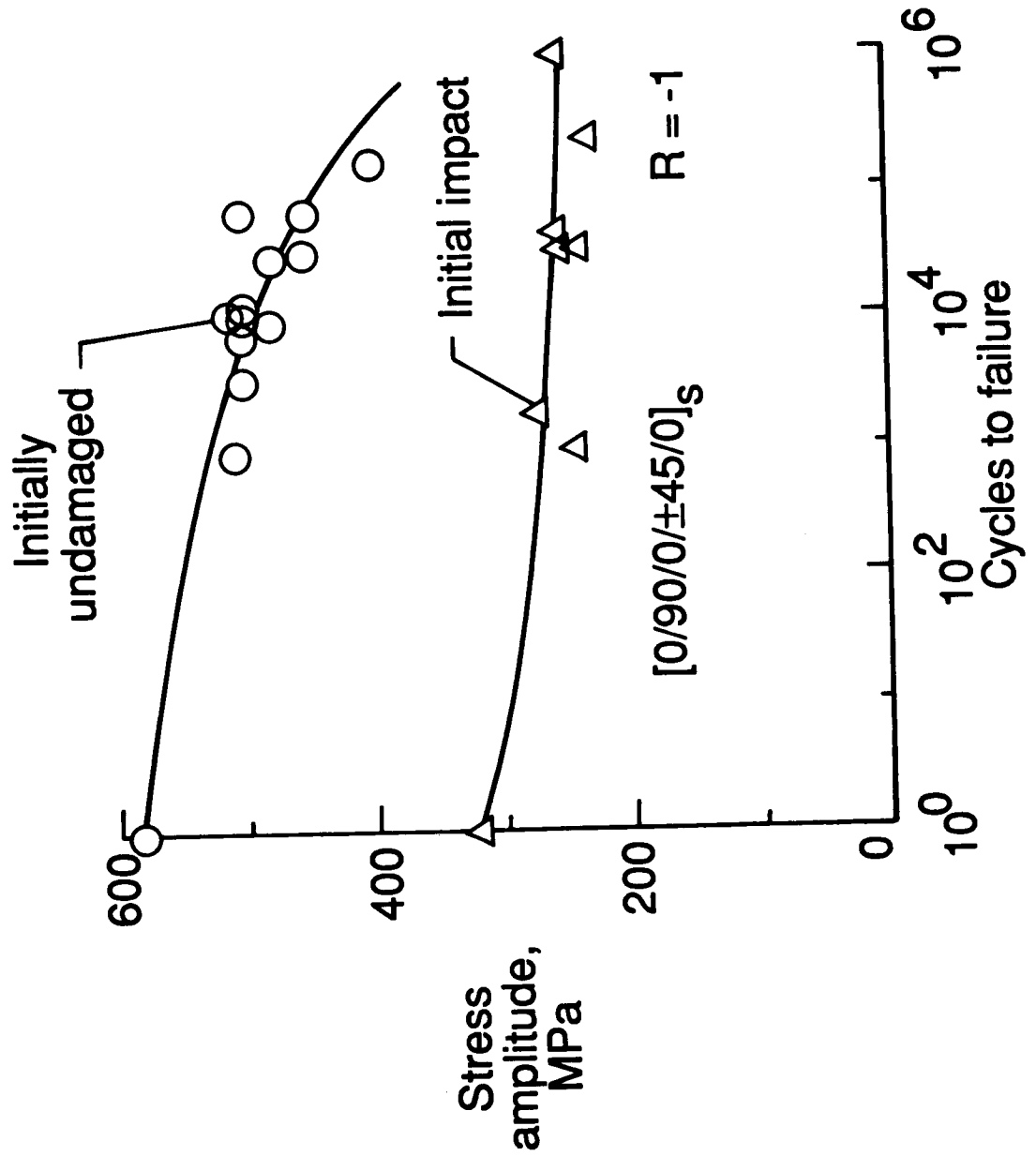


Figure 21. - Fatigue behavior of initially undamaged and impacted graphite epoxy laminates under fully reversed cyclic loading.

(45/0/-45/90) 5S T300/3501-6

1/2 inch spaced Kevlar stitch

320,973 cycles to failure

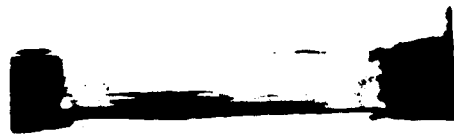
$$\sigma_{\max} = 60\% \sigma_{ult}$$

$$R = \frac{-32.5 \text{ ksi}}{-3.25 \text{ ksi}} = 10$$

0.31 in.  
thickness



320,00  
cycles



320,876  
cycles



320,933  
cycles

Figure 22. - Radiograph of through-the-thickness damage.

1. Report No. USAAVSCOM TM NASA TM-100548 88-B-009		2. Government Accession No.		3. Recipient's Catalog No.	
4. Title and Subtitle TOWARDS A DAMAGE TOLERANCE PHILOSOPHY FOR COMPOSITE MATERIALS AND STRUCTURES				5. Report Date March 1988	
				6. Performing Organization Code	
7. Author(s) T. Kevin O'Brien				8. Performing Organization Report No.	
9. Performing Organization Name and Address NASA Langley Research Center, Hampton, VA 23665-5225 and U.S. Army Aviation Research and Technology Activity (AVSCOM) Aerostructures Directorate, Langley Research Center, Hampton, VA 23665-5225				10. Work Unit No. 505-63-01-05	
				11. Contract or Grant No.	
12. Sponsoring Agency Name and Address National Aeronautics and Space Administration Washington, DC 20546-0001 and U.S. Army Aviation Systems Command St. Louis, MO 63120-1798				13. Type of Report and Period Covered Technical Memorandum	
				14. Army Project No.  1L161102AH45C	
15. Supplementary Notes  T. Kevin O'Brien, Aerostructures Directorate, USAARTA-AVSCOM, Langley Research Center, Hampton, Virginia.					
16. Abstract A damage-threshold/fail-safety approach is proposed for ensuring that composite structures are both sufficiently durable for economy of operation, as well as adequately fail-safe or damage tolerant for flight safety. Matrix cracks are assumed to exist throughout the off-axis plies. Delamination onset is predicted using a strain energy release rate characterization. Delamination growth is accounted for in one of three ways: either analytically, using delamination growth laws in conjunction with strain energy release rate analyses incorporating delamination resistance curves; experimentally, using measured stiffness loss; or conservatively, assuming delamination onset corresponds to catastrophic delamination growth. Fail-safety is assessed by accounting for the accumulation of delaminations through the thickness. A tension fatigue life prediction for composite laminates is presented as a case study to illustrate how this approach may be implemented. Suggestions are made for applying the damage-threshold/fail-safety approach to compression fatigue, tension/compression fatigue, and compression strength following low velocity impact.					
17. Key Words (Suggested by Author(s)) Damage tolerance Threshold Fail-safe Composite materials Delamination			18. Distribution Statement  Unclassified - Unlimited Subject Category - 24		
19. Security Classif. (of this report) Unclassified		20. Security Classif. (of this page) Unclassified		21. No. of Pages 63	22. Price* A04